Modeled Tsunami in Lake Washington from hypothetical ruptures on the Seattle Fault

Kathryn Richwine

A report prepared in partial fulfillment of
The requirements for the degree of

Master of Science
Earth and Space Sciences: Applied Geosciences

University of Washington

March 2020

Project Mentor:
Carrie Garrison-Laney, Washington Sea Grant

Reading Committee
Juliet Crider
Steven Walters

Message Technical Report Number: 084

Executive Summary

Tsunami deposits from an earthquake on the Seattle fault have been found around the Puget Sound area. Tsunami modeling has been conducted in Puget Sound with the Seattle fault as the initiating event, however published modeling efforts have not investigated the effects of an event from the Seattle fault on the Lake Washington area. The Seattle fault crosses Lake Washington extending east towards Lake Sammamish, and a tsunami generated from this fault could create hazardous conditions along the lake's shorelines. The parameters of the Lake Washington section of the Seattle fault are applied to create deformation files modeling potential tsunami waves generated from a fault rupture. Four simulations are run with the modern-day lake level and again with the pre-ship canal lake level using the open source software GeoClaw. These eight simulations are analyzed to determine which fault parameters produce a wave that inundates the shoreline. A scenario modeling a 10-meter slip at a depth of 1-km that uses the pre-ship canal lake level and a four-hour runtime determines the extent of inundation and locates potential areas for tsunami deposits. These results show that the shoreline is inundated four times over the first four hours after the earthquake, with maximum tsunami wave heights of 2 m to nearly 4 m arriving within minutes to tens of minutes of the fault rupture. I identify seven low-lying areas susceptible to inundation and suggest three sites for paleotsunami investigation as a test for these models. More extensive modeling of different scenarios and fault parameters is needed to understand the range of possible or likely inundation from a tsunami wave in Lake Washington triggered from the Seattle fault.

List of Figures

List of Tables

Acknowledgments

Many thanks to my outside mentor, Carrie Garrison-Laney, and to Randy LeVeque for the support in learning a new software and working through new model parameters. This project would not have been a success without their expertise.

Introduction

Lake Washington is a large, glacially carved lake located east of downtown Seattle and surrounded by major urban and suburban development (Figure 1). The Seattle Fault is an active thrust fault zone that transverses Lake Washington and Puget Sound. Tsunami deposits have been located around Puget Sound that are linked to earthquakes on the Seattle fault (Atwater and Moore, 1992; Atwater, 1999; Sherrod, 2000; Arcos, 2012). It is plausible that the Seattle fault could also generate large waves within Lake Washington.

Currently, no published models are available for a tsunami wave generated in Lake Washington. This research explores several aspects of a Lake Washington tsunami generated by hypothetical slip on the Seattle fault. I show that a Seattle fault rupture that offsets the floor of Lake Washington area could potentially create a serious hazard to the general public and to the infrastructure due to inundation from a large wave in the lake. Numerous houses are within proximity of the shoreline, the lake also acts as a major recreation area and the 520 floating bridge spanning the lake is traversed by hundreds of people daily, potentially placing thousands of people at risk in the result of a tsunami. Lake levels were ten feet higher prior to construction of the Lake Washington ship canal: modeling a pre-ship canal lake level event can give possible locations to look for deposits of past tsunami events. I present results of eight tsunami model scenarios using both modern-day lake levels and pre-ship-canal lake levels, to evaluate the potential impacts of a Seattle-fault-triggered tsunami on the Lake Washington shoreline. Each model simulates one hour of water level and velocity following a fault rupture. I also include an extended scenario using the pre-ship-canal lake level, with the goal to identify areas for future research investigating tsunami deposits. The project entailed determining the appropriate scenarios for fault ruptures and modeling tsunami waves that could impact the shoreline of the lake. Tsunami modeling uses the program GeoClaw (Clawpack, 2019), a subset of the Clawpack software package, plots and scenario videos were created with the program. The results presented are illustrative of the range of possible Lake Washington tsunamis, but they are not intended to be used as a specific prediction or risk analysis for properties or infrastructure on Lake Washington today.

Background

Seattle lies in a tectonically active area, with the Seattle fault zone (SFZ) traversing the city and Lake Washington. The Seattle fault is an active, south dipping, high angle, thrust fault zone with significant uplift occurring during an earthquake around 900 AD (Johnson et al., 1999, Atwater, 1999; Sherrod et al., 2000). A M_w ~7.3 earthquake is interpreted to be the cause of 23 feet of uplift south of the fault and a tsunami in Puget Sound in the past 1700 years (Buckman et al., 1992; Atwater and Moore, 1992). Although the Seattle area experiences earthquakes with a magnitude of 6.5 or larger about every 30-50 years (SFESPT, 2005), these events occur deep below Earth’s surface, on the subducting Juan de Fuca plate (Ludwin et al., 1991). Only in the last 20 years is there recognition that the region is vulnerable to near-surface earthquakes as well: geologists have discovered six active surface fault zones able to generate an earthquake much larger and more damaging, with one of those areas being the SFZ (Brocher et al., 2001; ten Brink et al., 2002; Blakely et al., 2002; Liberty and Pratt, 2008; Kelsey et al., 2008; Pratt et al., 2015).

Lake Washington is a large, 210-foot-deep lake that fills a former glacial trough. Natural drainage into Lake Washington consists of lowland creeks and rivers (Karlin and Abella, 1996). Once the lake was connected to Puget Sound through a canal and locks system (constructed in 1916), the lake level lowered by approximately ten feet to its current elevation of 23 feet above mean sea level. Lake drainage now occurs west through the ship canal into Lake Union rather than south to the Black River in Renton (Karlin and Abella, 1996).

Evidence of past tsunami and earthquake activity through tsunami deposits, uplift events, marsh stratigraphy, liquefaction and underwater forests have been found throughout the Puget Sound and Lake Washington area (Atwater and Moore, 1992; Atwater, 1999; Bucknam et al., 1992; Jacoby et al., 1992; Karlin and Abella, 1992; Sherrod et al., 2000; Martin and Bourgeois, 2012). Although most deposits have been linked to large megathrust earthquakes, some are related to waves generated by deformation along the Seattle fault and subsequent landsliding (Atwater and Moore, 1992; Atwater, 1999; Martin and Bourgeois, 2012). Tsunami deposits and liquefaction dating to 1100 years ago have been found in the Snohomish delta, Gorst, the Skokomish delta, and Lynch Cove (Martin and Bourgeois, 2012). Underwater forests created through massive block landslides are found in Lake Washington (Karlin and Abella, 1992 and 1996; Atwater and Moore, 1992). The upright drowned trees are linked to tsunami deposits located at West Point through high-resolution tree ring dating by Jacoby et al. (1992) in association with the 1100 earthquake event (Karlin and Abella, 1996). Atwater (1999) refined the most recent regional uplift event age to be 1100 year ago through tsunami deposits generated by an earthquake on the Seattle fault and

Sherrod et al. (2000) used sea-level rise data to confirm from Restoration Point marsh that this uplift event is the only such event in the past 7000 years.

Prior work has modeled the effects of a Seattle Fault earthquake on Puget Sound costal sites. The National Oceanic and Atmospheric Administration (NOAA) Center for Tsunami Mapping Efforts (TIME) conducted models in 2003 to map inundation in Puget Sound resulting from a major earthquake on the Seattle fault (Titov, et al., 2003). The MOST numerical model, based on long-wave approximation, is a finite-difference numerical algorithm. Significant inundation is found around Elliott Bay, with a maximum displacement of 19 feet (Titov, et al., 2003). The NOAA Tsunami Research Center modeled inundation around Tacoma and Everett to asses natural hazard mitigation using a M_w 7.3 earthquake on the Seattle fault (Venturato et al., 2007; Chamberlin and Arcas, 2015). The Seattle fault scenario by Venturato et al. (2007) records a maximum uplift value of 8 meters in the vicinity of south Bainbridge Island with maximum wave amplitudes of 3.5 meters reaching Commencement Bay and Gig Harbor about 19 minutes after the earthquake. Chamberlin and Arcas (2015) show that a M_w 7.3 earthquake displaces more water than a M_w 6.7 earthquake due to the larger seismic slip with inundation affecting Naval Station Everett, Jetty Island, and low-lying areas north of the Snohomish River. Additionally, Koshimura et al. (2002) modeled a M_w 7.6 earthquake generated by the Seattle fault linked to field evidence of the 1100 AD event to reproduce and validate tsunami modeling. The modeling demonstrated a tsunami wave can reach Cultus Bay in 20 minutes at mean high water but modeling the scenario at mean low water the tsunami wave does not reach the marsh at the head of Cultus Bay, where a sand layer attributed to the event is located. The inundation also does not cover the full extent of the sand deposit found by Atwater and Moore (1992) which may be a result of using modern day topography and near shore bathymetry that does not match up with past conditions (Koshimura et al., 2002).

Although tsunami research has been conducted around Puget Sound and coastal cities, no model results have been published for the Lake Washington area. There are several cities with business districts in low-lying areas around the Lake: Kenmore, Juanita, Kirkland, Bellevue, Renton and the University of Washington. Much of the rest of the shoreline comprises multi-million-dollar homes within meters of the shore. A 2006 study by Koshimura et al. presents a method for predicting casualties due to a tsunami inundation flow. The method uses a Tsunami Casualty Index (TCI) to compute at each grid point the location and times in a tsunami zone when evacuation is not possible and casualties are likely to occur (Koshimura et al., 2006). The data can be applied to population densities to improve evacuation routes and identifying areas to avoid. More research is needed to determine the extent of tsunami hazards on Lake Washington, to determine the size of a tsunami wave, and extent of inundation in the highly residential and urbanized area.

Seattle Fault Subsurface Geometry

The specific geometry of the SFZ is not well understood. The surface expression of the fault is obscured by recent glaciation, dense vegetation and urban development. Geophysical studies provide some constraint on the geometry of the fault. Magnetic anomalies define the trace of the Seattle fault (Blakely et al., 2002) and 3D seismic tomographic studies define seismic velocities below the Puget Lowland to a depth of 11 km but provide insufficient spatial resolution to define the subsurface geometry (Brocher et al., 2001). Seismic reflection data from several studies help to define the position and extent of fault strands (Yount and Gower, 1991; Prunier et al., 1996; Johnson et al., 1999; Blakely et al., 2002) but these data penetrate only to shallow depths (Johnson et al., 1999) and the deeper reflection lines lack vertical control (Johnson et al., 1994; Pratt et al., 1997). Kelsey et al. (2008) proposes a conceptual model of the SFZ to be a double vergent wedge thrust fold which may provide insight into the Seattle basin development. Folding earthquakes can occur hours to thousands of years after the last event and could be precursory to the next earthquake event (Kelsey et al., 2008).

The consensus understanding shows that the Seattle fault is an east-west trending zone consisting of several, parallel, south dipping, high-angle reverse faults (Pratt et al., 1997; Pratt et al., 2015; Blakely et al., 2002; ten Brink et al., 2002; Kelsey et al., 2008; Liberty and Pratt, 2008). The eastern extent of the SFZ is unknown because of absent marine waterways and limitations of early land-based seismic surveys, however, high resolution land seismic reflection profiles by Liberty and Pratt (2008) indicate the deformation front of the SFZ extends to at least 8 km east of Vasa Park (located on the western shoreline of Lake Sammamish). Moreover, the SFZ is observed near Lake Sammamish, across Lake Washington near Mercer Island and through Puget Sound to Bainbridge Island, with at least three strands of the fault crossing Lake Washington (Figure 2; Karlin, 1997).

The position and number of fault strands crossing Lake Washington have been investigated through seismic reflection studies (Yount and Gower, 1991; Prunier et al., 1996; Johnson et la., 1999; Blakely et al., 2002). Seismic reflection profiles collected on the west side of Mercer Island show evidence of a 5-km wide deformation zone and uplift that is bounded by Quaternary depocenters to the north and south (Johnson et al., 1999). Researchers infer from the Lake Washington seismic profile data that a northern Seattle fault strand extends along the strike of the local gravity anomaly towards eastern Puget Sound (Johnson et al., 1999). This northern fault is suggested to extend east through southern Lake Sammamish by Yount and Gower (1991) which is consistent with Prunier et al. (1996) seismic reflection profiling data (Johnson et al., 1999). In the northernmost splay, the hanging wall locally includes steeply north dipping alluvial fans and fluvial deposits from the Miocene Blakely Harbor Formation between 70-80° (Johnson et al., 1999). Blakely et al. (2002) presents a newer high-resolution aeromagnetic survey of the Puget Lowland that defines three main strands of the SFZ with marine seismic reflection profiles. They find the traces of the SFZ to be subparallel to mapped bedrock trends over a 50 km distance below Puget Sound, downtown Seattle and Lake Washington.

The research defining the Seattle fault dip provides a range of values (Johnson et al., 1994 and 1999; Pratt et al., 1997; Calvert and Fisher, 2001; ten Brink et al., 2002; Liberty and Pratt, 2008). A mean dip of 45-60° is proposed for the top 6 km of the fault and 45-65° for the top 1 km by Johnson et al. (1994, 1999) based on industry and high-resolution seismic reflection data. Pratt et al. (1997) proposes a dip of 45° for the top 6 km that shallows to 20-25° at depths of 6-16 km based on different industry data (ten Brink et al., 2002). Based on P-wave velocities from seismic reflection data, Calvert and Fisher (2001) proposes a dip of 60° for the top 1 km. Liberty and Pratt (2008) propose the main fault to dip at about 40° based on their research mapping the Vasa Park fault and concluding that the Vasa Park fault must intersect the main fault at depth. This results with the main fault dipping shallower than the Vasa Park fault, which could dip as little as 55º S. Research by ten Brink et al. (2002) suggests a fault dip range of 35-45º to a depth of 7 km with seismic reflection and refraction data, and this range cannot be constrained further as the dislocation model provides a dip of 35-50º fitting to the observed shoreline uplift.

The Seattle fault slip rate is loosely constrained. Using the offset of the Crescent Formation between the footwall of the Seattle fault zone and the surface, a total minimum slip of 10 m is estimated (ten Brink et al., 2002). This value cannot be constrained further with the most recently published data because of the unknown amount of Crescent Formation rock erosion from the hanging wall (ten Brink et al., 2002). Based on erosion rates and assuming an age of 1.9 Ma of the lowest Quaternary strata in central Puget Sound, Johnson et al. (1999) proposes a minimum Quaternary slip rate on the northern splay of about 0.6 mm/yr. However, assuming an age of 1 Ma for the Quaternary strata suggest a range of 0.7-1.1 mm/yr which may indicate a change of rate through time (Johnson et al., 1999). Assuming a 49º dip on the northern fault splay, Johnson et al. (1999) calculate 9.0-14.1 m of uplift is permissible due to the change of rate through time, which is consistent with Thorson (1996, Fig. 6).

Several paleoseismology studies provide constraints on earthquake history of the Seattle Fault. Nelson et al. (2003) look at the earthquake history at the Toe Jam Hill fault and conclude through examining five trenches propose the first radiocarbon earthquake recurrence for crustal faults in western Washington. Three to possibly four earthquakes are recorded in the strata between 2500 to 1000 years ago with the most recent event identified at the 900-930 AD earthquake and subsequent tsunami in Puget Sound (Nelson et al., 2003). The vertical deformation associated with the 900 AD event suggests an earthquake magnitude of M7 due to the >36 km long surface rupture (Nelson et al., 2003). A more recent study by Nelson et al. (2014) use scarp data to link a moderate earthquake event on the Seattle fault to M5.5-6.0 and a large event to M6.5-7.0. Sherrod et al. (2000) relates earthquake recurrence on the Seattle fault to relative sea level changes recorded at Restoration Point through diatom and plant seed assemblages. The marsh record dates to 7500 years ago and records three events linked to uplift trigger by the Seattle fault or beach berm accretion/erosion with the last event indicating 7 m of uplift linked to the 1000 cal yr B.P. event (Sherrod et al., 2000). The slip-per-event estimated on the main Seattle fault is not calculated as more research is needed to positively identify the smaller events recorded in the marsh stratigraphy (Sherrod et al., 2000). The estimated magnitudes for earthquakes on the Seattle fault provide only a range of values as, more research is needed to constrain the current estimates.

Seattle Fault Model Parameters

To model tsunamis in Lake Washington, I must first select a geometry and slip magnitude for a modeled Seattle fault. For this study, I choose a simple rectangular fault that crosses the Lake and extends the full width of the model domain, consistent with Johnson et. al (1999). The trace of the modeled fault corresponds with strand A from Johnson et al. (1999). I chose a fault dip of 40ºS. This value is within the bounds of the most recent research and it is an approximate average of the values presented by ten Brink et al. (2002) and in agreement with Liberty and Pratt (2008). According to Brocher et al. (2001), the Seattle fault extends to at least 13 km depth before tomographic data becomes unreliable with the top 9 km displaying the best imaged data. Extent, map trace, and dip are held constant for all scenarios.

With the models, I evaluate the effect of changing three parameters: 1) amount of fault slip, 2) depth of the top of the fault, and 3) water depth. In the model, slip is applied uniformly over the fault. I chose to model to end-member scenarios: a slip of 1 m, representing a moderate earthquake (M~6.8) and slip of 10 m, representing a very large earthquake (M~7.5). There is not yet consensus whether the top of the primary strand of the Seattle fault breaks the surface or is several kilometers below. In this report, I present results for each of the two slip scenarios on a modeled fault that a) breaks the surface, or b) terminates 1 km below the surface. Finally, these scenarios are run with modern lake level and again at the pre-ship canal lake level. The modern lake level scenarios are intended to explore the possible extent of the modern tsunami hazard around the lake, while the pre-ship canal scenarios are intended to identify potential areas to investigate for tsunami deposits.

Clawpack Software and GeoClaw Tsunami Model

GeoClaw is a subset of Clawpack, an acronym for “Conservation Laws Package” (LeVeque and Li, 1994; Clawpack, 2019). The GeoClaw branch of Clawpack originated out of a PhD dissertation by David George (2006). The software has been verified and validated through extensive testing and is a validated tsunami model by the U.S. National Tsunami Hazard Mitigation Program (NTHMP) (Gonzalez et al., 2015).

GeoClaw solves the two-dimensional shallow water equations, also known as the St. Venant equations, which are commonly used for modeling tsunami waves and inundation (Gonzalez et al., 2015). The shallow water equations are partial differential equations that introduce the fluid depth $h(x, y, t)$ and two horizontal depth-averaged velocities $u(x, y, t)$ and $v(x, y, t)$. Manning's coefficient, a variable for roughness, is held constant at 0.025 for tsunami modeling (LeVeque et al., 2011). Coriolis terms can be added to the equation, but these have been found negligible in tsunami modeling (LeVeque et al., 2011) and are not used for the Lake Washington study.

The tsunami model initial conditions are based on the idea that lake level elevation is a simplified representation of the static lake bottom and the vertical displacement due to a seismic event. Tsunami generation time is small, on the order of minutes, compared to tsunami periods, on the order of tens of minutes, so that the seismic event is considered instantaneous (Hammack, 1972). The modern-day lake level is set to 3.1 meters above mean high water (MHW) while the pre-ship-canal lake level scenarios set the lake level to 6.1 m.

Model Limitations and Uncertainties

Models do not produce simulations of natural processes without error. The greatest source of error in this study is produced from interpreting the geologic evidence for an earthquake source. As one of the first studies to focus on a seismic event to produce a tsunami wave in Lake Washington, I chose geologically plausible but loosely constrained and highly simplified representations of the fault geometry, position, and slip. As research narrows the bounds of uncertainty on the Seattle fault zone, the model scenarios will increase accuracy.

Several other factors were not addressed that could influence tsunami propagation and inundation. The modeling of landslides triggered by earthquake shaking around Lake Washington was not included in this study. The impact of landslides could increase inundation around the lake; however, landslides are outside the scope of this project. The Manning's coefficient of friction set to n=0.025 is a standard for tsunami modeling in representing a gravelly, bare earth (LeVeque et al., 2011), however, a larger value is more representative in areas with vegetation that generally reduce the amount of inundation. The GeoClaw model computes with a spatially constant value 'n' even though a spatially variable coefficient of friction would yield more accurate results. The software requires more development to include this change of surface roughness throughout the study area. Structures along the lake were also not included in the model. The absence of buildings along the shore can significantly alter the speed and depth of tsunami inundation on shore. Larger tsunamis create a debris field that can multiply the destruction and expends the energy of the tsunami. This would decrease the inland extent of inundation (Gonzalez et al., 2015). The scouring and deposition that occurs during the tsunami is not accounted for in the modeling. This aspect can alter the flow and wave heights of the tsunami and reduces the extent of inundation by expending more energy through the movement of material (Gonzalez et al., 2015).

Methods

GeoClaw is an open source program that can be downloaded via the website www.clawpack.org/geoclaw. For this study, the software was run with Windows 10 on a PC laptop. I used the operating system Ubuntu, an open source Linux distribution program, to run the code. For GeoClaw to install and run properly, Anaconda3, a free and open-source distribution of Python was downloaded and installed, utilizing Python 3.7. Within the Anaconda3 suite, the subset Jupyter Notebook was used for developing deformation files and creating the study area boundary conditions.

Download and Installation

A tar file of the most recent Clawpack release was downloaded from the website: https://github.com/clawpack/clawpack/releases and untarred with the command *tar -xzf clawpack-v5.6.1.tar.gz*. The software was installed with the command *pip install --user -e .* and then exported to the working directory with *export CLAW=/full/path/to/clawpack-v5.6.1*. Before testing the install, the environments for Clawpack and Python need to be set in the .bashrc file. To do so, navigate the folder of the .bashrc file and use the command *nano .bashrc* to edit the file. The environment variables CLAW and PYTHONPATH need to be set to the same working folder. Once the environments are set, the paths can be tested with the commands *echo $PYTHONPATH* and *echo $CLAW*. These should read out the same path set in the .bashrc file. GeoClaw can now be tested by running sample scenarios that have been included with the install. Once these are run and checkout, the program is ready to be used. Some features not yet available with the most recent version of Clawpack v5.6.1 are needed to run scenarios in the Lake Washington area found at the website https://github.com/clawpack/new_features_for_v5.7.0. The 'new features for v5.7.0' folder is required for Lake Washington modeling.

Boundary Conditions

Jupyter Notebook is an open-source web application used to create and share documents that contain live code and data visualizations. Working with Randy LeVeque I created a notebook to produce deformation files for several Seattle fault scenarios. The notebook also contains the code to define the study area of Lake Washington, downloading the topography file for the area and to define the fixed grid monitoring points. The Jupyter Notebooks are available as an electronic appendix to this report.

Topography File

The 1/3 arc second topo file was downloaded from NOAA's National Geophysical Data Center's (NGDC) website and read into the MakeInputFiles_LakeWA notebook (Figure 3). The puget_sound_13_mhw_2014.nc, which extends across Lake Washington, is the standard file used for all tsunami modeling projects around the Puget Sound area (pers. comm. Randy LeVeque). By using this file, the results from this study can be applied to future work pertaining to tsunami modeling in the Greater Seattle area. The extent of the topo file is bounded by the coordinates: -122.45, -122.1, 47.39, 47.81, covering the entire study area, both water and land, incorporated in the study.

Fixed Grid Monitoring

GeoClaw can monitor certain points on a 'fixed grid' through interpolating from the adaptive mesh refinement (AMR) grids at specified time steps. This allows the user to record maximum flow depth, maximum flow velocity, momentum or momentum flux at certain points (LeVeque et al., 2011). The arrival time at each specified point can also be recorded to track the wave timing and movement. The fixed grid does not have to be a rectangular grid with coordinate directions but can consist of a list of points that are located along a one-dimensional transect or shoreline. The fgmax_points for Lake Washington are defined with a list of points which decreases processing times because the list omits large areas of land where the tsunami wave will not reach.

Define boundary between Puget Sound and Lake Washington

A boundary condition is set to separate Puget Sound from Lake Washington at the Ballard Locks. This condition selects the fgmax points for the grid. This is also where the initial lake elevation is set greater than the initial sea level (mean high water, MHW) in Puget Sound, because both the modern-day lake level and the pre-ship canal lake levels are above MHW. The coordinates defining the boundary from the sound and the lake are listed in Figure 4. The boundary created between Puget Sound and Lake Washington is converted into a ruled rectangle, enclosing the lake, and including all the fgmax points that are defined in the notebook (Figure 5). With the ruled rectangle defined, points are selected with an elevation below sea_level_lake (to select all the points in the lake) and to march outward and include a buffer_width onshore that includes points regardless of topography (Figure 6). The buffer width for all scenario runs is set to 10, selecting all points within 10 meters of the shoreline regardless of elevation change. The grid is then set with z_{max}=15 to include all points around the shoreline at the elevation less than 15 meters (Figure 7). These boundary conditions now define all fgmax points to include all points in Lake Washington and all points around the lake that are within 10 meters of the shore and all areas with at most 15 meters of elevation. The fgmax points are exported to create the input file fgmax_pts_LakeWA.data for scenario runs using the modern-day lake level and the input file fgmax_pts_LakeWA_precanal.data for scenario runs using the pre-ship canal lake level (Figure 8).

The ship canal between the Ballard Locks and Portage Bay are included in all model runs. This was done because adding the area does not increase processing time by much, making the Ballard Locks a boundary creates a good landmark to end the defined area. Also, since the ship canal has not been modelled before, generating results for the area is an easy addition that can provide background information for future work. To keep the model simplified, the pre-ship canal scenarios also include the modern-day ship canal boundary conditions. The boundary at the Ballard Locks simulates a wall by not letting water flow out of the locks and water from the sound to flow in. This can cause water to 'pile' up in the area which can lead to generating higher flows back through the ship canal close to the locks. Keeping the western extent defined at the locks, takes this issue out of the pre-ship canal scenarios.

Deformation File Generation

The Jupyter Notebook MakeInputFiles_LakeWA creates the deformation files (also known as the dtopo file) for all earthquakes simulated. The notebook reads in the parameters set in Figure 9. Changing the slip value and the depth value creates the .tt3 files needed for model run inputs. The code is run for the lake level set to 3.1 m for the modern-day scenarios or set to 6.1 m for the pre-ship canal scenarios. This creates all eight deformation files run in the test scenarios (Table 2).

Gauge Locations

Gauge locations are specified as single point locations (x, y). The locations are used to better visualize the solution behavior at that single point. The gauge locations can be used as a comparison to physical tidal gauges or pressure gauges located in the study area or to compare results with different methods or grid resolutions (Clawpack, 2019). I selected between 4- and 11-gauge locations for the each of the north, south, and middle areas of Lake Washington, as well as Lake Union and the ship canal to record wave properties (Figures 10-13). The gauge locations were chosen based on population, recreation areas close to the shoreline, low-lying shoreline, deep bathymetry, and narrow passage locations encompassing Lake Union.

The northern area of Lake Washington includes five model gauges. (Fig. 10). The low-lying waterfront at Kenmore (gauge #101) is the northern most gauge in the study area with gauge #100 just offshore. Matthew’s Beach (gauge #104) is low lying and is a popular attraction in the Sandpoint area of the Lake. Juanita Beach Park (gauge #102) is a low-lying area on the east side of Lake Washington that could be susceptible to inundation and gauge #103 is just offshore. The deepest area in the north Lake Washington grid (gauge #105) is located to report wave speed and height.

The middle Lake Washington area has seven-gauge locations (Fig.11). The Kirkland Waterfront gauge #201 and the Yarrow Point gauge #203 are selected for their lower elevation and its higher population density than surrounding areas on the east side of the lake. Gauge #200 is located at Magnuson Park for its low elevation and as a popular attraction for recreation. Gauge #205 is located on the shoreline of the Union Bay Natural Area, which is another low-lying location and a popular destination for recreation and gauge #206 is in the middle of Union Bay. Gauge #204 is in Fairweather Bay, on the east side of the lake to record wave properties. Gauge #202 located in the middle of the lake is in the deepest area for this section to record wave speed and height.

The south Lake Washington area has 11-gauge locations (Fig. 12). The populated areas of Bellevue (gauge # 300 and 301) and Renton (gauge # 310 and 311) both have a gauge on their shoreline to record wave speed and height in these higher populated areas and another gauge located off the shoreline to record the on-coming wave speed and height. Gauge #309 is located on the western shoreline of Lake Washington at Parkshore Marina, a low-lying and popular recreation destination. Gauge #305 is situated at the northeast coast of Mercer Island, where strong wave speeds are recorded. Gauge #308 is selected to record wave properties at the south end of Mercer Island and Gauge #306 to record the west side of Mercer Island. Gauge #307 is in Andrews Bay, where waves tend to pile up due to the orientation of the mouth to Andrews Bay. Gauge #303 and 304 were added after a test run since this is allow-lying area and is inundated by the simulated tsunami wave.

Five gauges are in the Lake Union and Portage Bay grid (Fig. 13). Gauge #405 is located at the entrance of the Fremont Cut into Lake Union to record wave speed and height from the restricted waterway into the lake. Gauge #402 and 404 are located within Lake Union on the shoreline. Gauge #402 is located on the shore of Gas Works Park, a low-lying area and a popular recreation area and Gauge #404 is located on the shore of South Lake Union at Lake Union Park, another low-lying area and popular recreation destination. Gauge #401 is located within the ship canal between the I-5

Bridge and the Eastlake Bridge to record wave speed and height at the constricted ship canal bend. Gauge #400 is located at the entrance of Portage Bay to Montlake Cut to record wave speed and height as it enters a narrow passageway.

Scenario Run Set-up

The setrun.py file is set up to define the number of output files generated, the time interval for the file generation, the boundary conditions that have already been defined above, number of refinement levels, all gauge data and the time each gauge will begin recording data, which deformation file is being used, the topo file, the lake level elevation and several other adjustments to calculations. When all parameters have been changed accordingly, the code is run in Ubuntu with the command *make .data*. The software will run several checks on the parameters and create a list of files with the extension .data. When the command is run successfully (without any error warnings), the scenario can be run to create output files at the specified time intervals. The command *make .output* is utilized and the code will run until all output files have been created and are generated in the _output folder.

The setplot.py file can be set up to plot the output files. Specifications include creating zoomed-in areas of interest, changing scales and plotting colors. The file is run with the command *make plots* and will generate a video of the scenario along with all gauge data that plots the gauge depth, wave speed and wave height versus time at all gauge locations specified in the set run.

Trial Scenarios

Eight trial scenarios were run to evaluate which fault parameters have the greatest effect on the study area. These results were evaluated to determine which scenario to select for an extended model run. The eight scenarios were run for a model duration of one-hour, which required about 10 hours processing time for each run. Output files were created at a model-time interval of every two minutes, to generate 30 output files for each trial run. Plots were created, averaging eight additional hours of processing time to create one video and all gauge plots for each scenario.

Extended Scenario Run

Given the amount of computing time to generate output files and to plot the results, just one scenario from the test runs was selected for an extended scenario run. The scenario selected for the longer run is the 10-meter slip at 1-kilometer depth for the pre-ship canal lake level. A scenario at depth instead of breaking the surface was chosen because this seems like a more probable option for the Seattle fault. The pre-ship canal lake level was selected for the possibility that these results can highlight areas around Lake Washington to investigate for possible paleotsunami deposits. Scenarios with a 10-meter slip generated a large wave that is within the bounds of a large earthquake for the Seattle fault. The 1-meter slip scenarios generated a much smaller wave. I elected the larger slip with the larger wave in order to investigate the possible tsunami inundation generated by a very large earthquake. The scenario was run for a 4-hour model time period and produced 36 output files. Output files were created every five model-minutes for the first two hours and every 10 model-minutes for the last two hours. The processing time to create the output files was 48 hours, with 12 hours to plot the results.

Results

Trial Scenarios Results

The trial scenarios display a difference in displacement and uplift from the 1-meter slip versus the 10-meter slip simulations. All 1-meter slip scenarios generate a wave that is at its maximum less than 0.7 meters in height and with a maximum speed of 1.02 m/s (Tables 3-4, Figures 14, 18-19). While the wave created is small on Lake Washington and up to 0.59 meters of uplift recorded on land in the southern area of the Lake, inundation is minimal.

The water level-change south of the Seattle fault is instantaneous at time=0, with 5.65 meters increase if the fault rupture is at the surface and 5.92 meters increase with a fault rupture at 1 km depth (Tables 3-4). The initial wave produces a 2.8-meter surface wave elevation traveling north. That wave reaches its maximum speed at t=0.2 hours (12 minutes after the earthquake) for a surface rupture or around 0.4 hours (24 minutes), for the rupture at depth (Figure 18). The maximum wave speed for the surface rupture scenario records a faster wave speed (0.822 m/s) during the initial 30 minutes of the event, while the scenario at 1 km depth records faster wave speeds (0.978 m/s) during t=0.4 hours to t=1.0 hours. The 10 meters slip scenarios generate a larger wave, producing higher wave heights and faster maximum wave speeds with both the modern-day and pre-ship canal lake levels.

Modern Day Lake Level Runs Summary

Table 3 presents the summary of the maximum wave properties for the modern-day lake level scenarios. The initial tsunami wave elevation data for time two minutes and four minutes after the event are shown in Figures 14-17. Transect 1 crosses the fault and extends north to Juanita Bay while transect 2 is located south of the fault. The transects illustrate the difference of initial wave elevation for the four scenarios run with the modern-day lake level. The 10-m slip scenarios record larger initial uplift south of the fault and generates a larger initial wave compared to the 1-m slip scenarios. The blind scenarios illustrate a more diffuse initial wave compared to the surface-breaking scenarios.

The maximum surface elevation of the lake through time for each scenario is presented in Figure 18. Three of four scenarios run with the modern-day lake level record maximum water height at gauge 307 in Andrews Bay (near Seward Park, Seattle). The 10-meter slip with a fault rupture at the surface, records a maximum surface elevation 0.1 meters higher at gauge 311 (in Renton).

The maximum wave speed locations for the 1-meter slip scenarios with the modern-day lake level are recorded at gauge 400, at the mouth of the Montlake Cut into Portage Bay (Figure 19). The 10-meter slip scenarios record their maximum wave locations in south Lake Washington with the fault rupture at the surface recording its maximum speed at gauge 306 (west of Mercer Island) and the fault rupture at 1 km depth located at gauge 305 (East Channel).

The two highest maximum flow values (greatest flux) for all four scenarios are recorded at gauges 105 (deepest area in the northern section of Lake Washington) and

202 (deepest area in the middle section of Lake Washington). Gauges 301 (Meydenbauer Bay) and 306 (East Channel) record high flow depth areas for all four scenarios (Figure 20).

Pre-ship Canal Lake Level Trials Summary

Table 4 presents the summary of the maximum and minimum wave properties for the scenarios run with the pre-ship canal lake level.

The initial tsunami wave elevation data for the pre-ship canal lake level scenarios are comparable to the modern-day lake level scenarios with the exception that the pre-ship canal scenarios record at a higher initial lake level (Figures 21-22). The 10-m slip scenarios illustrate an initial wave elevation of approximately 2 m propagating northward. The blind scenarios show a more diffuse wave compared to the surface-breaking scenarios. The transect graphs for the 1-meter slip scenarios with the pre-ship canal lake level display data representative of the modern-day lake level scenarios seen in Figure 14 and are omitted from the report.

Extended Scenario Results

I selected one scenario to run for four-model hours: 10 m fault slip on a blind (1 km-deep) fault with pre-ship-canal lake levels to produce 36 output files at a time interval of every five minutes for the first two hours and every 10 minutes for the third and fourth hours. Table 5 presents the summary of the extended run scenario maximum and minimum wave properties. This scenario was run to identify areas around Lake

Washington that may contain tsunami deposits from past earthquakes on the Seattle fault.

Areas of modeled inundation by gauge data are plotted in Figure 24 These locations are plotted at higher resolution in Figures 25-28. In this scenario, low lying areas are inundated by more than 1 m of water up to four times, over the course of four hours. Maximum wave speeds at these locations are commonly higher than 1 m/s.

The maximum wave speeds are recorded at the northeast corner of Mercer Island with high wave speeds east of Mercer Island that inundate the shoreline in the low-lying area of Mercer Slough Nature Park, located south of Bellevue (Figure 23). Maximum wave speeds are also recorded west of Mercer Island in conjunction with the initial uplift. Six areas are identified for potential tsunami deposits located from the maximum depth onshore map (Figure 24). Gauge data is taken from the gauges identified in Figure 24 to include surface wave elevation data, the number of inundations, and the maximum wave speed at these locations.

South Bellevue

The area with the most extensive modeled inundation is South Bellevue. Gauges 303 and 304 were added to the run after a test run indicated the low-lying area of the Mercer Slough Nature Park is susceptible to inundation. The Newport Yacht Club and 0.75 km inland is inundated with 1.5-meters of water, which extends northward through the nature preserve to a half-meter of inundation (Figure 25). Gauge 303 records a high of 1.8 meters surface wave elevation at t=1.0 hours while gauge 304 records a high of 1.9 meters surface wave elevation at t=1.0 hours (Figure 25). The surface wave elevation time series indicate four inundation events over the four-hour time period, with the second event recording the highest water elevation level.

Kenmore

In the northern extent of Lake Washington, Kenmore's waterfront and the mouth of the Sammamish River indicates a large area of inundation. Gauge 101 records 3.9 meters surface elevation at t=0.5 hours, the highest water elevation level for the four largest inundation events (Figures 24 and 26). Inundation north of the Sammamish River is less than 0.5 km and south of Sammamish River, at its longest extent, less than 0.4 km and reaching 8.3 km downriver to the Woodinville area (Figure 26).

East Side

The east side of Lake Washington has several bays and the surrounding shoreline inundated including the Kirkland Waterfront, Yarrow Bay, Cozy Bay and Fairweather Bay (Figure 27). Gauge 204 in Fairweather Bay records the highest surface wave elevation level with a value of 3.4 meters, followed by Yarrow Bay (203) with 3.1 meters and the Kirkland Waterfront (201) with 2.4 meters of surface wave elevation inundation (Figure 24). The furthest extent inland is at Yarrow Bay with 0.6 km. All three gauges report the highest surface wave elevation within the first half hour, however, gauge 204 indicates a larger first inundation event compared to gauges 203 and 201 with many rapid waves (Figure 27).

Juanita Beach Park

The last location of inundation on the east side of Lake Washington is Juanita Beach Park. Gauge 103 reports 2.7 meters of surface wave elevation at the shoreline with the first wave reaching the area in the first 20 minutes (Figures 24 and 28). Juanita Beach Park is inundated four times in the four-hour runtime with the inundation reaching 0.9 km in the southern extent and 0.5 km in the northern extent (Figure 28).

Sandpoint Region

Matthews Beach Park, gauge 104, and Magnuson Park, gauge 200, report 3.1 meters and 2.2 meters of surface wave elevation inundation, respectfully, occurring at t=0.5 hours (Figures 24 and 28). Both gauge locations are inundated four times. Matthews Beach Park is inundated up to 0.4 km from the shoreline. The northern portion of Magnuson Park is inundated inland by 0.4 km and by 0.8 km at the southern portion of the park (Figure 28).

University of Washington, Union Bay Natural Area

The Union Bay Natural Area on the campus of the University of Washington is a low-lying area reported to be susceptible to inundation with the high surface wave elevation data of 2.2 meters at gauge 205 (Figures 24 and 28). The initial wave reaches the area at t=0.3 hours and records one maximum inundation event followed by two smaller events in the first four hours (Figure 28). The maximum extent of inundation reaches 1.3 km inland.

Renton

Renton, located at the most southern extent of Lake Washington is instantaneously flooded due to the uplift and susceptible to inundation with the high surface wave elevation data of 5.1 meters at gauge 310 and 5.6 meters at gauge 311 (Figures 24 and 29). The maximum inundation event occurs at t=0 with three more inundation pulses of 2 m and smaller recorded at gauge 311 (Figure 29). The maximum extent of inundation reaches 2.8 km inland.

Overall, the inundation along the shoreline of Lake Washington ranges inland a horizontal distance of 20 meters to 150 meters in areas not highlighted in the seven regions for potential tsunami deposits.

Discussion

The test scenarios lay the groundwork to begin to understand what parameters affect tsunami modeling in Lake Washington from an event triggered by the Seattle fault. The depth of the rupture may create differing wave speed signatures. The scenarios with a fault rupture at depth create a more diffusive wave throughout the lake while the blind scenarios create a more pronounced wave propagating through the lake.

The maximum flow depths for all eight scenarios are similar (Tables 3-4). These values are recorded at gauges located in deeper water at gauges 105 (Deepest Area, North), 202 (Deepest Area, Middle), 301(Meydenbauer Bay), and 306 (West of Mercer Island) with gauges 105 and 202 recording the highest flow depth for all scenarios at t= 0.5 hours (Figure 20). This may be because the lake is deep enough that the difference between a large tsunami wave and a small one is still a small fraction of the original water depth.

The maximum surface elevation plots for seven scenarios is recorded at the same gauge, gauge #307, Andrews Bay; where the 1-meter slip scenarios record the largest surface wave elevation change at around 14 minutes after the earthquake and the 10-meter slip scenarios record their highest value with the initial uplift at t=0 and a second highest value at 14 minutes after initiation (Figure 18). Andrews Bay may be recording the highest surface elevations due to the orientation of mouth of the bay relative to the Seattle fault and allowing the water to accumulate with higher wave speeds. The 10-meter slip scenario with a fault rupture at the surface, records a maximum surface elevation 0.1 meters higher at gauge 311 (in Renton).

The trial scenarios demonstrate that changing the fault slip results in greater wave-property changes compared to differences seen when changing the fault rupture depth, among the tested scenarios. The differences between the 10-meter slip scenarios for the modern-day lake level and the pre-ship canal lake level are minimal with the exception that the pre-ship canal surface wave elevation values are three meters higher to start, resulting in more extensive inundation. This finding suggests that, to reduce uncertainty in tsunami hazard estimates, it is more important to focus on studies that examine differing fault slip values rather than the fault rupture depth. This study does not examine the effect different positions of the modeled fault; initial trials not reported here suggest that the position of the fault rupture relative to Mercer Island will have a significant influence on the tsunami waves.

This study highlights seven areas for potential tsunami deposit investigation: South Bellevue, Kenmore, East Side, Juanita Beach Park, Sandpoint Region, the University of Washington: Union Bay Natural Area, and Renton. These seven areas are all low-lying coastal areas that are predominately nature preserves (South Bellevue, East Side bays, Juanita Beach Park, Sandpoint Region, and the Union Bay Natural Area) or waterfronts (Kenmore, Juanita, East Side south of Kirkland, and Renton). The Union Bay Natural Area, although now a nature preserve, is a site of an old landfill.

Given this information, the Union Bay Natural Area is not an ideal place to investigate for paleotsunami deposits. Urbanized or highly developed waterfront areas are also unlikely to host preserved paleotsunami deposits.

The original extended run did not capture the entire scenario and a longer run was set up to cover eight hours of model time with 52 output files for every five minutes for the first two hours, every ten minutes for hours three and four and every 15 minutes for the remaining four hours. The eight-hour run did not model to the end of the scenario; however, it captures the most significant inundation events within the first four hours and continues to capture the scenario to inundation events decreasing to 0.5 m or less for all discussed areas.

The number of inundation events at the six areas north of the fault (excluding Renton) are consistent. with four main events in the first four hours of runtime. Exceptions are gauge 304 located in the Mercer Slough Nature Park and gauge 205 located in the Union Bay Natural Area. The differing inundation events for gauge 304 may be attributed to the increased wave speed around the northeastern corner of Mercer Island creating a larger wave propagation in the immediate area and resulting in two inundation events that are more diffuse compared to the four distinctive inundation events seen at the other areas (Figure 25). The three inundation events recorded at gauge 205 illustrate another area with a more diffusive wave propagation which may be a result of the orientation of Union Bay to the direction of the incoming and outgoing waves (Figure 28). The remaining four areas: Kenmore, Juanita Beach Park, Sandpoint Region and East Side (excluding gauge 303 south of Bellevue) are directly on the shoreline of Lake Washington with comparable inundation events. With all areas, excluding the South Bellevue gauges, the first inundation event is the strongest, while the South Bellevue gauges record the second inundation event as the strongest event (Figures 25-28). This may be attributed to the wave speed and the narrow passageway at the northeastern corner of Mercer Island.

All gauges (excluding the South Bellevue gauges) record a surface wave elevation between 2.2 and 3.9 m, with Kenmore recording the highest value (Figure 24). Located at the most northern extent of Lake Washington, the Kenmore area may be a good area to look for tsunami deposits. Given the surface wave elevation data recorded at gauge 101, the mouth of the Sammamish River and surrounding area could provide the right environment for preserving tsunami deposits as a low-lying and undeveloped area (Figure 25). Moreover, Juanita Beach Park, Matthews Beach Park, Magnuson Park, and the East Side bays are all low-lying and relatively undeveloped areas of land, ideal for investigating tsunami deposits.

In the Sandpoint Region, the area south of gauge 200 appears to be more ideal for locating tsunami deposits compared to the Matthews Beach Park gauge 104 due to the higher wave speed recorded at Magnuson Park with 2.04 m/s versus the 0.61 m/s at Matthews Park Beach (Figure 24). The topography of the Sandpoint shoreline seems to reduce the wave speeds reaching Matthews Beach Park even though the inundation depths are higher (3.1 m at gauge 104 versus 2.2 m at gauge 200) (Figure 24).

On the East Side, Fairweather Bay may record a stronger inundation event for the three bays. Yarrow Bay, east of Fairweather Bay, records its maximum surface wave elevation at 3.1 m and a maximum wave speed of 1.38 m/s while Fairweather Bay records its maximum surface wave elevation at 3.4 m and a maximum wave speed of

2.01 m/s (Figure 24). The orientation of the mouth of Fairweather Bay could direct stronger wave speeds though the bay and create an environment for a stronger tsunami signal.

The South Bellevue gauges 303 and 304 record the most extensive inundation in the study area (Figure 25). The Mercer Slough Nature Park could be the area most likely to host tsunami deposits around Lake Washington due to its low-lying elevation, the undeveloped area and with almost two meters of inundation recorded throughout the preserve. Gauge 304 records the highest wave speeds out of all the identified areas with 6.05 m/s and gauge 303 records a maximum wave speed of 1.47 m/s south of Bellevue (Figure 24). The high wave speeds can potentially suspend and erode more material with the ability to transport more sediment to the area.

The maximum speed data points can help identify areas of erosion and transport using the Hjulstrom Curve. Gauges recording maximum speeds above 0.3 m/s show that the waves can entrain sand size particles , which would be deposited inland when the waves slow below 0.05 m/s. (Hjulstrom, 1935) High wave speeds at some location suggest that significant erosion could occur around the shoreline of Lake Washington (Fig. 23).

Water heights for all six sites inundated remain about 1 m above the initial lake level for the entirety of the runtime, even between waves. The land uplift south of the fault could have permanently changed the volume of the lake basin. This would create permanently higher lake levels everywhere, until water drains through the ship canal or other outlets. This suggests a risk for additional flooding along the canal and in Renton, where the natural outlet for the lake used to exist.

These findings are based on a limited number of scenarios of Seattle fault parameters. Changing one or more fault parameters may lead to differing results. More extensive sensitivity studies on the parameters of the Seattle fault are needed to understand more fully how changing parameters changes the effect of the resulting tsunami wave. In future studies, I recommend focusing on the effect of changes in slip and studying the position of the fault crossing Lake Washington. More studies focusing on the dip of the fault can also help with gaining insight of how much range this value can have on resulting tsunami waves.

Conclusions

In this report, I present modeled tsunami in Lake Washington from eight hypothetical earthquake scenarios on the Seattle fault. The variables I evaluated are: fault slip, fault depth and initial lake level variations. I find that greater slip produces a larger and faster wave than less slip; shallow ruptures makes more pronounced waves than deep rupture; and higher lake level makes little difference except for extent of inundation inland.

In all of the scenarios, the lakeshore is inundated instantaneously or within minutes. South of the fault, instant and persistent inundation is recorded for the duration of the runtime. North of the fault, repeated waves on top of persistent inundation of about 1 m is recorded for the duration of the runtime. Peak water velocities of 1 -6 m/s suggest the potential for erosion, sediment transport throughout most of the Lake Washington shoreline, especially in the area of the Mercer Slough Nature Preserve, Kenmore Waterfront and the mouth of the Sammamish River, Kirkland Waterfront, Renton Waterfront and Magnuson Park.

The extended model simulation of a large, blind earthquake at pre-ship-canal lake levels highlights several locations around Lake Washington that might host paleotsunami deposits from a large Seattle fault earthquake. The M_w 7.5 earthquake scenario models a possible event that may have occurred in the past and may potentially occur in the future. Although the shoreline is modified and densely developed, there remains several relatively undisturbed locations to investigate. These include: the mouth of the Sammamish River, Magnuson Park, Juanita Beach Park and Mercer Slough Nature Preserve.

In this modeling study, I did not evaluate many factors that could influence shoreline inundation, wave propagation, or related hazard. The model does not include direct effects of earthquake shaking, landslides and related bathymetric changes, bridges crossing the lake or the effect of shoreline infrastructure on the wave. I did not investigate various possibilities for fault position or dip, complex slip distributions, or the effect of multiple strands.

Generating tsunami models that consider variations in Seattle-fault geometry is an important aspect to address in future work. This project begins to lay the groundwork of relating geologic parameters to tsunami models. As research improves the error bounds on the Seattle fault geometry and slip history, scenarios based on the most recent research will improve accuracy. Bridging this gap between the modeling and geoscience communities will benefit not only the scientific community but can improve estimates of earthquake hazard.

As one of the first studies to analyze the Lake Washington area, I have illustrated how tsunamis can potentially create serious hazards for the general public and infrastructure on the water and the surrounding shoreline. Moreover, scenarios have highlighted areas to investigate tsunami deposits, offering the potential to constrain models with past earthquake and tsunami evidence. This study highlights the importance of expanding the coverage of tsunami modeling beyond Puget Sound and into Lake Washington, with several potential areas of inundation identified, including important transportation lifelines and densely populated areas.

References

Arcos, M.E.M., 2012, The A.D. 900-930 Seattle-fault-zone earthquake with a wider coseismic rupture patch and postseismic submergence; inferences from new sedimentary evidence: Bulletin of the Seismological Society of America, v. 102, no. 3, p. 1079-1098.

Atwater, B.F., 1999, Radiocarbon dating of a Seattle earthquake to A.D. 900-930, Seismological Research Letters, v. 70, p. 232.

Atwater, B.F. and Moore, A.L., 1992, A tsunami about 1000 years ago in Puget Sound, Washington, Science, v. 258, no. 5088, p. 1614.

Blakely, R.J., Wells, R.E., Weaver, C.S., and Johnson, S.Y., 2002, Location, structure, and seismicity of the Seattle fault zone, Washington: evidence from aeromagnetic anomalies, geologic mapping, and seismic-reflection data, GSA Bulletin, v. 114, no. 2, p. 169-177.

Bourgeois, J. and Johnson, S.Y., 2001, Geologic evidence of earthquakes at the Snohomish delta, Washington, in the past 1200 yr, GSA Bulletin, v. 113, no. 4, p. 482-494.

Brocher, T.M., Parsons, T., Blakely, R.J., Christensen, N.I., Fisher, M.A., Wells, R.E. and the SHIPS working group, 2001, Upper crustal structured in Puget Lowland, Washington: Results from the 1998 seismic hazards investigation in Puget Sound, Journal of Geophysical Research, v. 106, no. B7, p. 13,541-13,546.

Bucknam, R.C., Hemphill-Haley, E. and Leopold, E.B., 1992, Abrupt uplift within the past 1700 years at Southern Puget Sound, Washington, Science, v. 258, no. 5088, p. 1611-1614.

Calvert, A.J., Fisher, M.A., and SHIPS working group, 2001, Imaging the Seattle fault zone with high-resolution seismic tomography, Geophysical Research Letters, v. 28, no. 12, p. 2337-2340.

Chamberlin, C., and Arcas, D., 2015, Modeling tsunami inundation for hazard mapping at Everett, Washington, from the Seattle fault, NOAA Technical Memorandum OAR PMEL-147, p. i-18.

Clawpack, 2019, Clawpack software, www.clawpack.org.

George, D.L., Finite Volume Methods and Adaptive Refinement for Tsunami Propagation and Inundation. PhD thesis, University of Washington, 2006.

Gonzalez, F.I., LeVeque, R.J. and Adams, L.M., 2015, Tsunami hazard assessment of the strait of Juan de Fuca final report, University of Washington.

Hjulstrom, F., 1935, Studies of the morophological activity of rivers as illustrated by the River Fyris, Bulletin Geological Institute Upsalsa, v. 25, p. 221-527.

Jacoby, G.C., Williams, P.L. and Buckley, B.M., 1992, Tree ring correlation between prehistoric landslides and abrupt tectonic events in Seattle, Washington, Science, v. 258, p. 1621-1623.

J.L. Hammack. Tsunami - A Model of Their Generation and Propagation. Report No. KH-R-28, California Institute of Technology, Pasadena, CA, 1972.

Johnson, S.Y., Potter, C.J., and Armentrout, J.M., 1994, Origin and evolution of the Seattle basin and Seattle fault, Geology, v. 22, p. 71-74.

Johnson, S.Y., Dadisman, S.V., Childs, J.R. and Stanley, W.D., 1999, Active tectonics of the Seattle fault and central Puget Sound, Washington- implications for earthquake hazards, Geological Society of America Bulletin, v. 111, no. 7, p. 1042-1053.

Karlin, R.E. and Abella, S.E.B., 1996, A history of Pacific Northwest earthquakes recorded in Holocene sediments from Lake Washington, Journal of Geophysical Research, v. 101, no. B3, p. 6137-6150.

Karlin, R.E. and Abella, S.E.B., 1992, Paleoearthquakes in the Puget Sound region recorded in sediments from Lake Washington, U.S.A., Science, v. 258, p. 1617-1620.

Kelsey, H.M., Sherrod, B.L., Nelson, A.R. and Brocher, T.M., 2008, Earthquakes generated from bedding plane-parallel reverse faults above an active wedge thrust, Seattle fault zone, GSA Bulletin, v. 120, no. 11/12, p. 1581-1597.

Koshimura, S., Katada, T., Mofjeld, H.O., and Kawata, Y., 2006, A method for estimating casualties due to the tsunami inundation flow, Natural Hazards, v. 39, p. 265-274.

Koshimura, S., Mofjeld, H.O., Gonzalez, F.I., and Moore, A.L., 2002, Modeling the 1100 bp paleotsunami in Puget Sound, Washington, Geophysical Research Letters, v. 29, no. 20, p. 1948.

LeVeque, R.J., George, D.L. and Berger, M.J., 2011, Tsunami modelling with adaptively refined finite volume methods, Acta Numerica, Cambridge University Press, p. 211-289.

LeVeque, R.J., Finite Volume Methods for Hyperbolic Problems. Cambridge University Press, 2002.

LeVeque, R.J. and Li, Z., 1994, The immersed interface method for elliptic equations with discontinuous coefficients and singular sources, SIAM Journal on Numerical Analysis, v. 31, n. 4, p. 1019-1044.

Liberty, L.M. and Pratt, T.L., 2008, Structure of the eastern Seattle fault zone, Washington state: new insights from seismic reflection data, Bulletin of the Seismological Society of America, v. 98, no. 4, p. 1681-1695.

Ludwin, R.S., Slemmons, D.B., Engdahl, E.R., Zoback, M.D., Blackwell, D.D., Weaver, C.S., and Crosson, R.S., 1991, Seismicity of Washington and Oregon: Boulder, CO, Boulder, CO, United States: Geol. Soc. Am, 77 p.

Martin, M.E. and Bourgeois, J., 2012, Vented sediments and tsunami deposits in the Puget Lowland, Washington- differentiating sedimentary processes, Sedimentology, v. 59, p. 419-444.

National Oceanic and Atmospheric Administration, 2019, National centers for environmental information, https://www.ngdc.noaa.gov/maps/bathymetry/, accessed January 29, 2019.

Nelson, A.R., Personius, S.F., Sherrod, B.L., Kelsey, H.M., Johnson, S.Y., Bradley, L., and Wells, R.E., 2014, Diverse rupture modes for surface-deforming upper plate earthquakes in the southern Puget Lowland of Washington State: Geosphere, v 10(4), 769-796.

Nelson, A.R., Johnson, S.Y., Kelsey, H.M., Wells, R.E., Sherrod, B.L., Pezzopane, S.K., Bradley, L., Koehler III, R.D., and Bucknam, R.C., 2003, Late Holocene earthquakes on Toe Jam Hill, Seattle fault zone, Bainbridge Island, Washington, GSA Bulletin, v. 115, no. 11, p. 1388-1403.

Pratt, T.L., Troost, K.G., Odum, J.K., and Stephenson, W.J., 2015, Kinematics of shallow backthrusts in the Seattle fault zone, Washington state, Geosphere, v. 11, no. 6, p. 1948-1974.

Pratt, T.L., Johnson, S., Potter, C., Stephenson, and Finn, C., 1997, Seismic reflection images beneath Puget Sound, western Washington state: The Puget Lowland thrust sheet hypothesis, Journal of Geophysical Research, v. 102, no. B12, p. 27,469-27,489.

Prunier, C.F., Karlin, R.E., Holmes, M., and Pratt, T., 1996, Seismic landslides in Puget Sound (SLIPS) IV- Holocene neotectonics and mass wasting in Lake Sammamish related to the Seattle fault, Eos (Transactions, American Geophysical Union), v. 77, p. F500.

Seattle Fault Earthquake Scenario Project Team, 2005, Scenario for a magnitude 6.7 earthquake on the Seattle fault. Earthquake Engineering Research Institute, 1st ed., p. 162.

Sherrod, B.L., Bucknam, R.C., and Leopold, E.B., 2000, Holocene relative sea level changes along the Seattle fault at Restoration Point, Washington, Quaternary Research, v. 54, p. 384-393.

Ten-Brink, U.S., Molzer, P.C., Fisher, M.A., Blakely, R.J., Bucknman, R.C., Parsons, T., Crosson, R.S. and Creager, K.C., 2002, Subsurface geometry and evolution of the Seattle fault zone and the Seattle basin, Washington, Bulletin of the Seismological Society of America, v. 92, no. 5, p. 1737-1753.

Thorson, R.M., 1996, Earthquake recurrence and glacial loading in western Washington, Geological Society of America Bulletin, v. 108, p. 1182-1191.

Titov, V.V., Gonzalez, F.I., Mofjeld, H.O. and Venturato, A.J., 2003, NOAA TIME Seattle tsunami mapping project: procedures, data sources, and products, NOAA Technical Memorandum OAR PMEL-124, Contribution no. 2572, p. 21.

Venturato, A.J., Arcas, D., Titov, V.V., Mofjeld, H.O., Chamberlin, C.C. and Gonzalez, F.I., 2007, Tacoma, Washington, tsunami hazard mapping project: modeling tsunami inundation from Tacoma and Seattle fault earthquakes, NOAA Technical Memorandum OAR PMEL-132, Contribution no. 2981, p. 23.

Yount, J.C., and Gower, H.D., 1991, Bedrock geologic map of the Seattle 30’ by 60’ quadrangle, Washington, Geological Survey Open-File Report 91-147, p. 37, 4 plates.

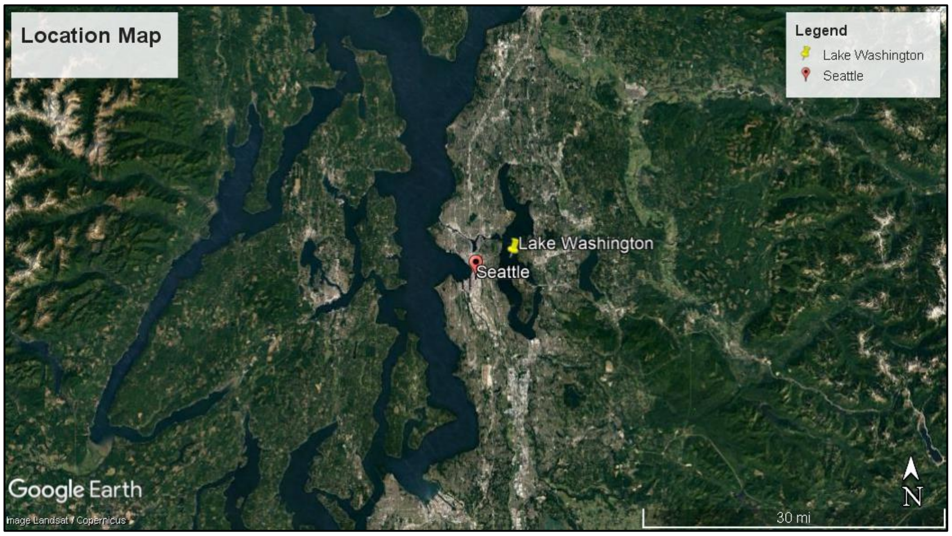

Figure 1. Location map. Lake Washington is east of downtown Seattle. Geographic information taken from GoogleEarth.

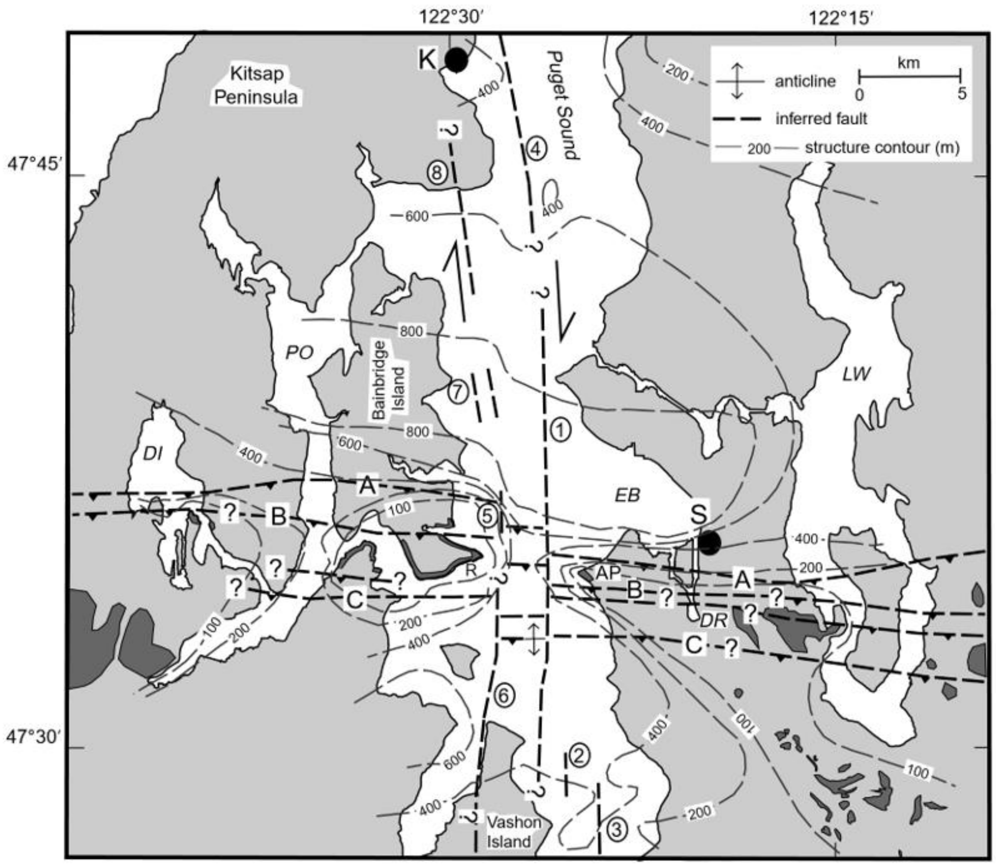

Figure 2. Map showing location of structures of the Seattle fault zone. Land is underlain by Quaternary deposits (light shading) with small areas underlain by Tertiary Rocks (dark shading). From Johnson, et al. (1999).

```
try:
    # read existing file
    topo_1_3sec = topotools.Topography()
    topo_1_3sec.read('input_files/topo_1_3sec_LakeWA.tt3')
    print('Read existing file')
except:
    try:
        extent = [-122.45, -122.1, 47.39, 47.81]
        path = 'https://www.ngdc.noaa.gov/thredds/dodsC/regional/puget_sound_13_mhw_2014.nc'
        topo_1_3sec = topotools.read_netcdf(path, extent=extent, verbose=True)
        topo_1_3sec.write('input_files/topo_1_3sec_LakeWA.tt3')
    except:
        # in case that fails:
        from clawpack.clawutil.data import get_remote_file
        print('Reading from thredds server failed, instead read cached version from geoclaw...')
        remote_topo_dir = 'http://depts.washington.edu/clawpack/geoclaw/topo/WA/'
        fname = 'topo_1_3sec_LakeWA.tt3'
        path = os.path.join(remote_topo_dir, fname)
        get_remote_file(path, output_dir='input_files', file_name=fname,
                        verbose=True)
        topo_1_3sec = topotools.Topography()
        topo_1_3sec.read('input_files/topo_1_3sec_LakeWA.tt3')
```
Figure 3. Code written in Jupyter Notebook to download the topography file from NOAA's NDGC website. The region extent of Lake Washington is defined with the 'extent' coordinates to cover the study area. The defined topography file is saved in the working folder as 'topo_1_3sec_LakeWA.tt3'.

```
ybdry = array([47.39,   47.46,  47.54, 47.60,      47.65,      47.68,    47.82])
xbdry = array([-122.2, -122.2, -122.3, -122.31, -122.3974, -122.3974, -122.28])
```

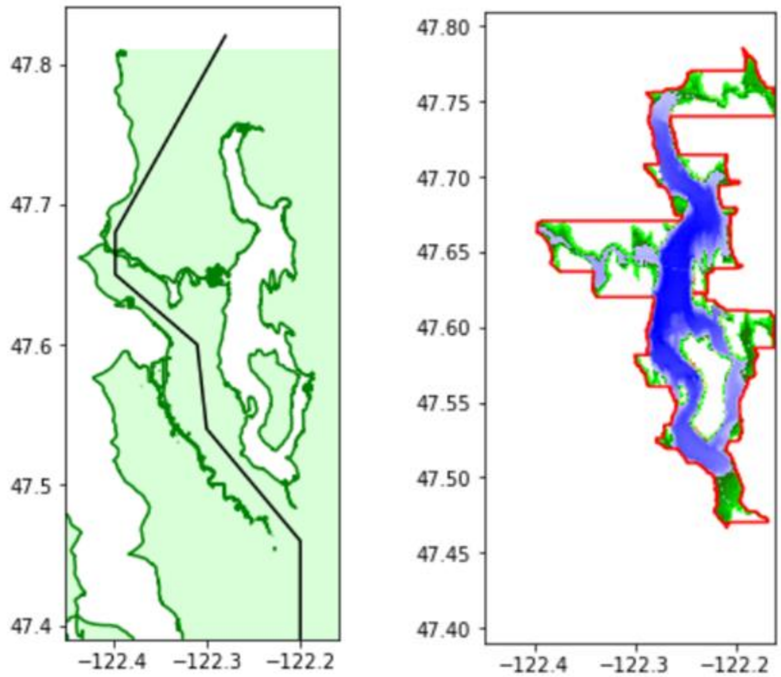

Figure 4. Defining the boundary between Puget Sound and Lake Washington is seen on the left. This boundary is used for selecting fgmax points and for setting the initial lake elevation to be greater than the initial sea level (MHW) in Puget Sound. The image on the right shows the 'ruled rectangle', which is the region that includes all fgmax points.

```
rr_lake = region_tools.RuledRectangle()
rr_lake.s = ybdry
rr_lake.lower = xbdry
rr_lake.upper = -122.16 * ones(xbdry.shape)
rr_lake.ixy = 'y'
rr_lake.method = 1
rr_lake_x, rr_lake_y = rr_lake.vertices()  # vertices of polygon
#rr_lake.write('input_files/RuledRectangle_Lake.data') # make a better one below for AMR
```

Figure 5. Code written in the Jupyter Notebook defining the ruled rectangle region for Lake Washington.

```
topo = topo_1_3sec
mask_out = rr_lake.mask_outside(topo.X, topo.Y)
buffer_width = 10
pts_chosen = marching_front.select_by_flooding(topo.Z,
                                               mask=mask_out,
                                               Z1=sea_level_lake,
                                               Z2=1e6,
                                               max_iters=buffer_width)
```
Figure 6. Code written in the Jupyter Notebook defining a buffer width around the lake set to 10. This selects all fgmax points within 10 meters of the shoreline regardless of elevation change.

```
Zmax = 15.
pts_chosen = marching_front.select_by_flooding(topo.Z,
                                                mask=mask_out,
                                                Z1=sea_level_lake,
                                                Z2=Zmax,
                                                prev_pts_chosen=pts_chosen,
                                                max_iters=None)
```

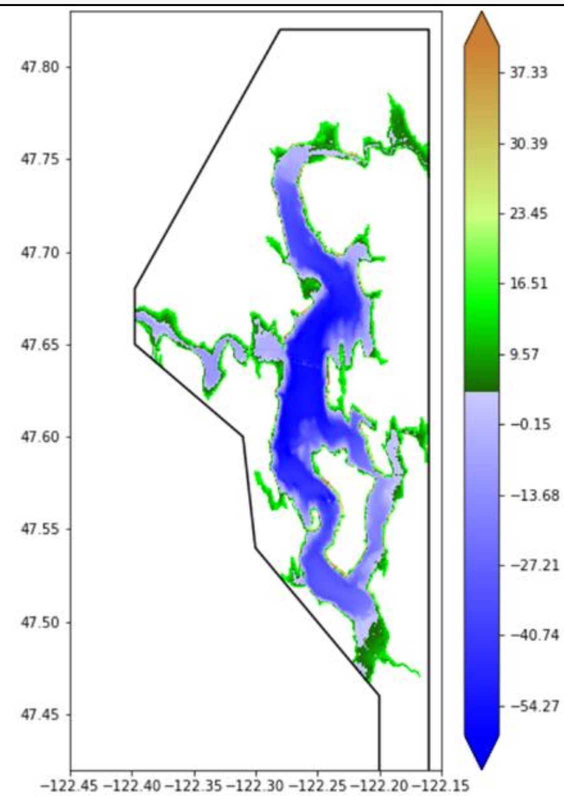

Figure 7. All fgmax points are selected that are less than 15 meters elevation or within 10 meters of the shore. The green colored fgmax points are locations on dry land and the blue colored fgmax points are location selected in the lake.

```
fname_fgmax_mask = 'input_files/fgmax_pts_LakeWA_precanal.data'
topo_fgmax_mask = topotools.Topography()
topo_fgmax_mask._x = topo.x
topo_fgmax_mask._y = topo.y
topo_fgmax_mask._Z = where(pts_chosen,1,0)
topo_fgmax_mask.generate_2d_coordinates()

topo_fgmax_mask.write(fname_fgmax_mask, topo_type=3, Z_format='%1i')
print('Created %s' % fname_fgmax_mask)
```

Figure 8. Code written in the Jupyter Notebook to convert the fgmax points selected for the study area into the input file for the pre-ship canal lake level that will be used to generate deformation files. This code is also used to create the input file for the modern-day lake level scenarios.

```
s = dtopotools.SubFault()

s.strike = 90.
s.dip = 40.
s.rake = 90.
s.slip = 1.
s.latitude = 47.57
s.longitude = -122.25
s.length = 20e3
s.width = 16e3 / cos(s.dip*pi/180.)
print('width = %.2f m' % s.width)
s.depth = 1.  # meters
s.coordinate_specification = 'top center'
s.calculate_geometry()
f = dtopotools.Fault()
f.subfaults = [s]
dtopo = f.create_dtopography(x,y,times=[1.]);
print('Mw = %6.2f' % f.Mw())
```

Figure 9. Code written in the Jupyter Notebook to set the fault parameters for each deformation file. Only the slip and the depth were changed for the differing scenarios run.

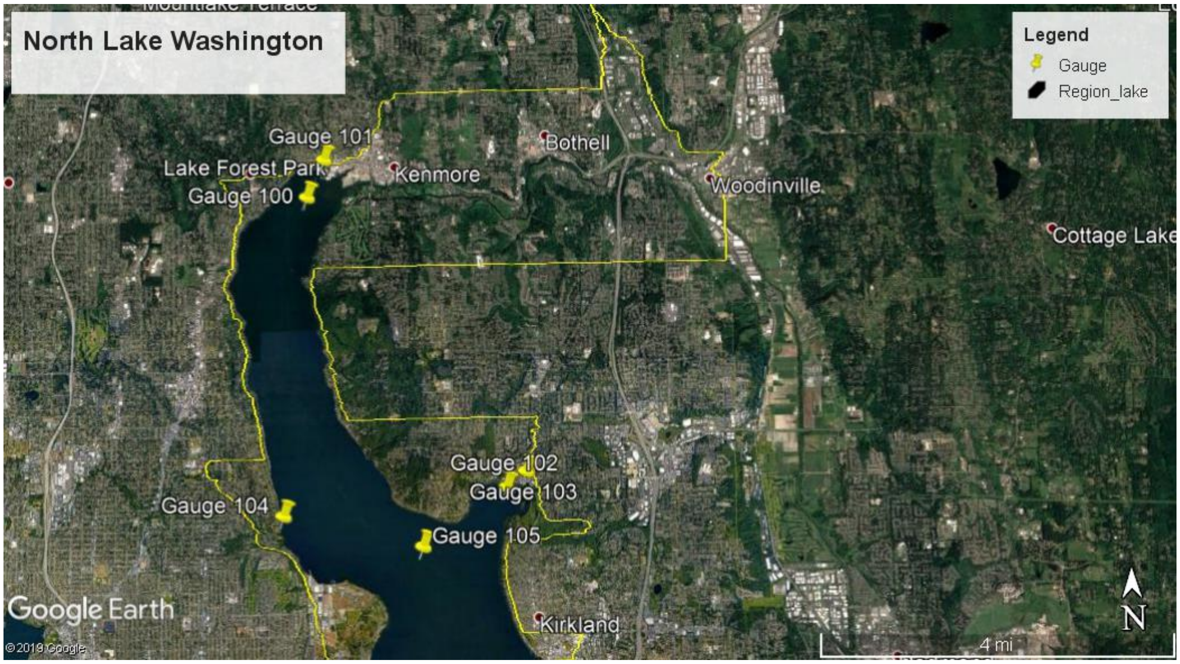

Figure 10. Gauge locations selected in the northern region of Lake Washington. These were utilized in all test scenarios run and the extended scenario run.

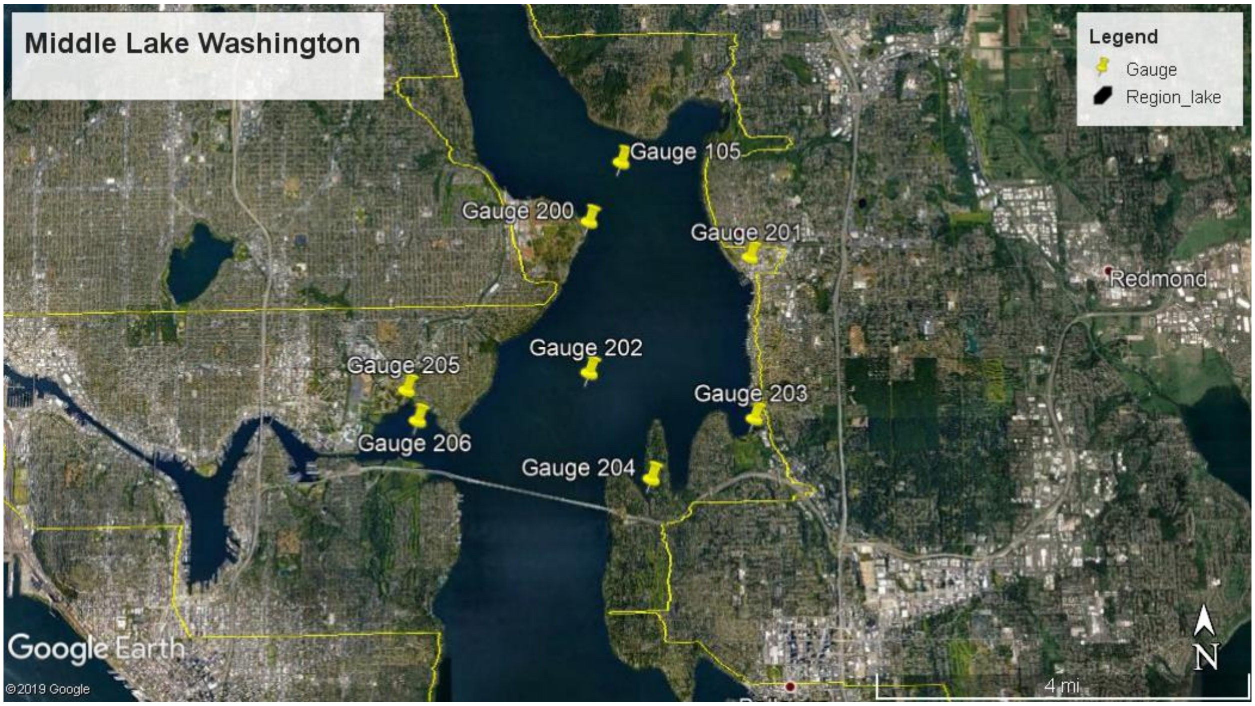

Figure 11. Gauge locations selected in the middle region of Lake Washington. These were utilized in all test scenarios run and the extended scenario run.

Figure 12. Gauge locations selected in the southern region of Lake Washington. These were utilized in all test scenarios run and the extended scenario run.

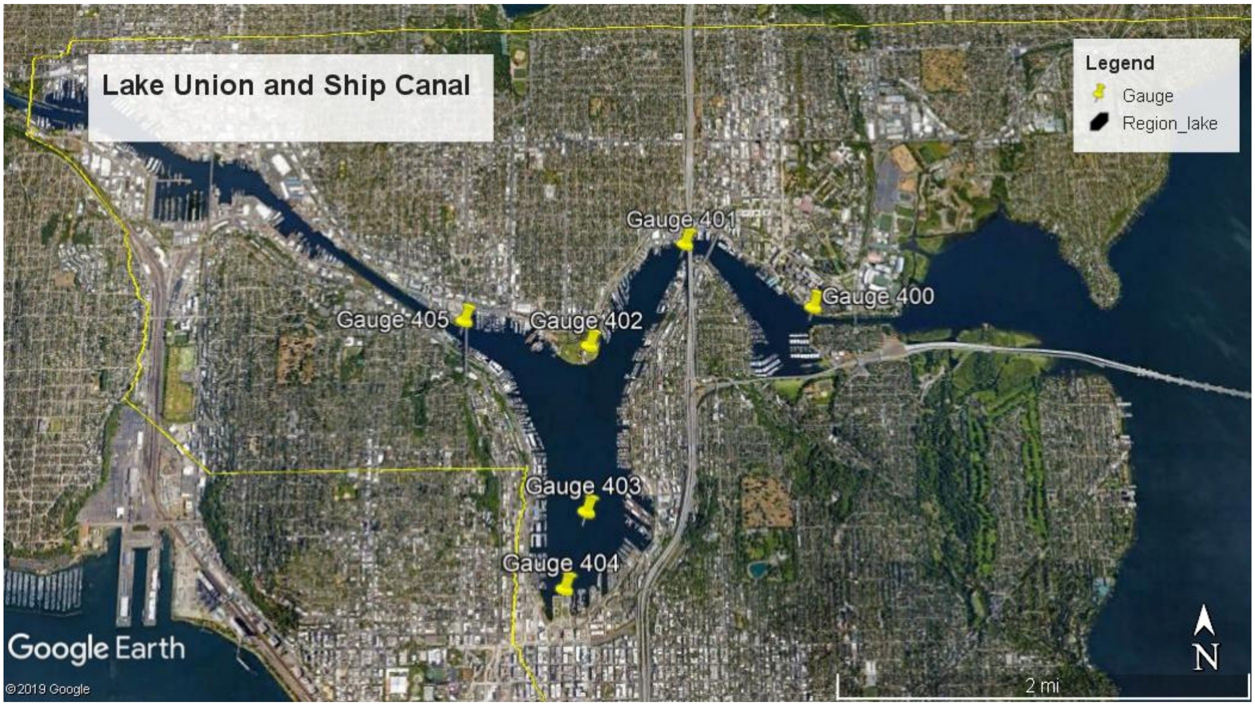

Figure 13. Gauge locations selected in the ship canal. These were utilized in all test scenarios run and the extended scenario run for consistency. Gauge data recorded in this region for the pre-ship canal lake level scenarios were not taken into consideration.

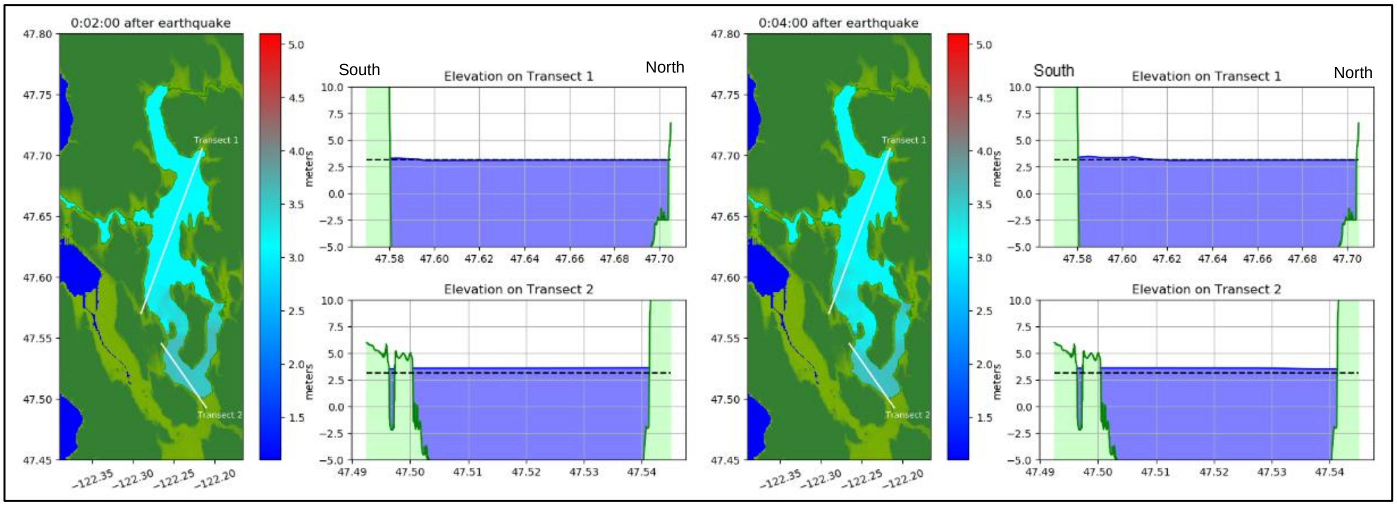

Figure 14. The 1-meter slip with a fault rupture at the surface scenario indicting surface wave elevation at t= 2 minutes on the left and t= 4 minutes on the right with an elevation of less than 0.5 meters north of the Seattle fault (Transect 1). Instantaneous uplift is seen south of the Seattle fault (Transect 2). The black dotted line indicates the initial lake level, set to 3.1 meters above MHW for the modern-day lake level.

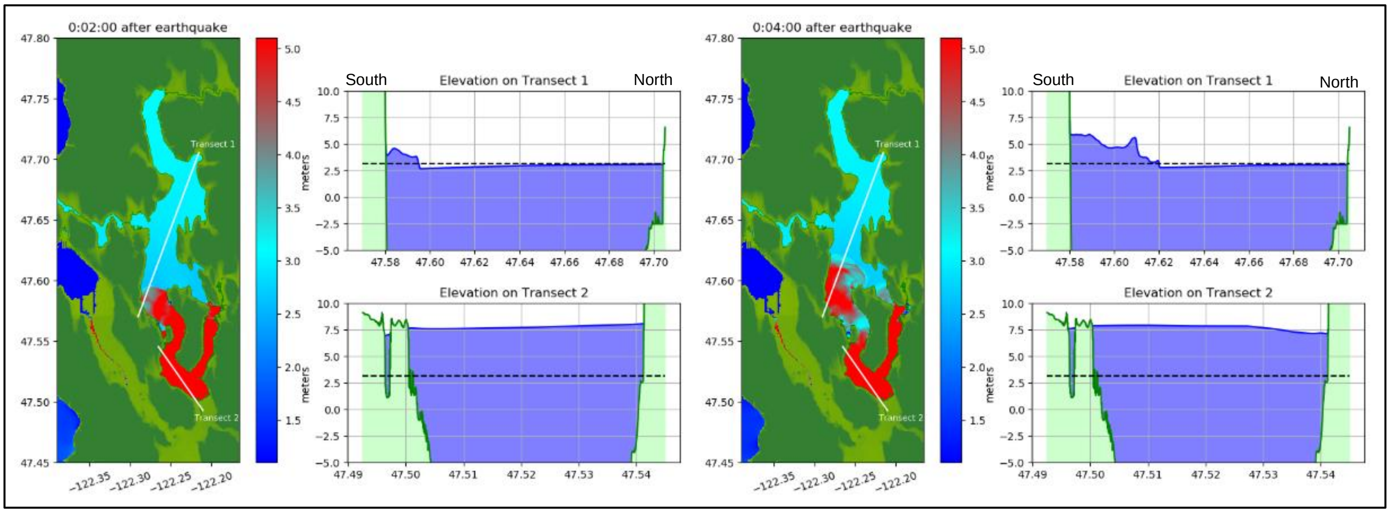

Figure 15. The 10-meter slip with a fault rupture at the surface scenario indicating surface wave elevation at t= 2 minutes on the left and t= 4 minutes on the right with an elevation of 2 meters north of the Seattle fault (Transect 1). Instantaneous uplift is seen south of the Seattle fault (Transect 2). The black dotted line indicates the initial lake level, set to 3.1 meters above MHW for the modern-day lake level.

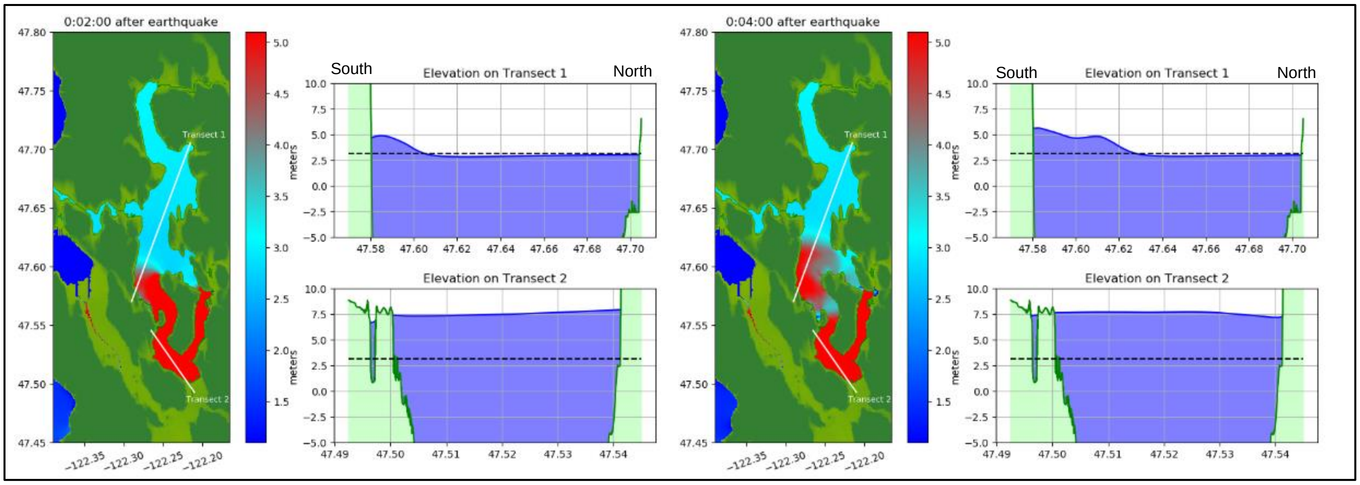

Figure 16. The 10-meter slip with a fault rupture at a depth of 1 km scenario indicating surface wave elevation at t= 2 minutes on the left and t= 4 minutes on the right with an elevation of 2 meters north of the Seattle (Transect 1). Instantaneous uplift is seen south of the Seattle fault (Transect 2). The black dotted line indicates the initial lake level, set to 3.1 meters above MHW for the modern-day lake level.

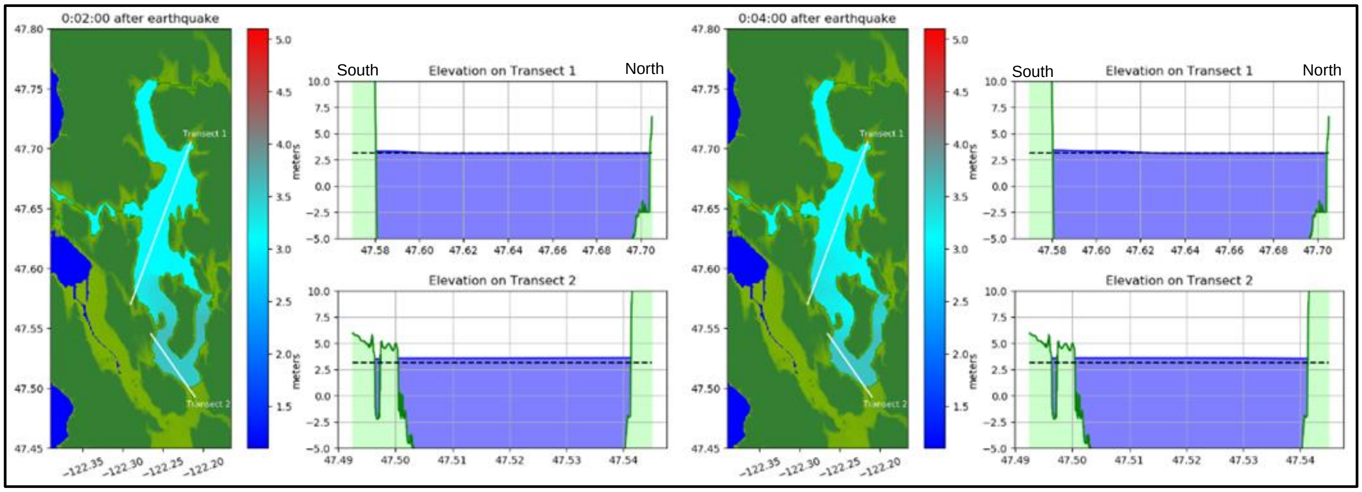

Figure 17. The 1-meter slip with a fault rupture at 1km depth scenario indicting surface wave elevation at t= 2 minutes on the left and t= 4 minutes on the right with an elevation of less than 0.5 meters north of the Seattle fault (Transect 1). Instantaneous uplift is seen south of the Seattle fault (Transect 2). The black dotted line indicates the initial lake level, set to 3.1 meters above MHW for the modern-day lake level.

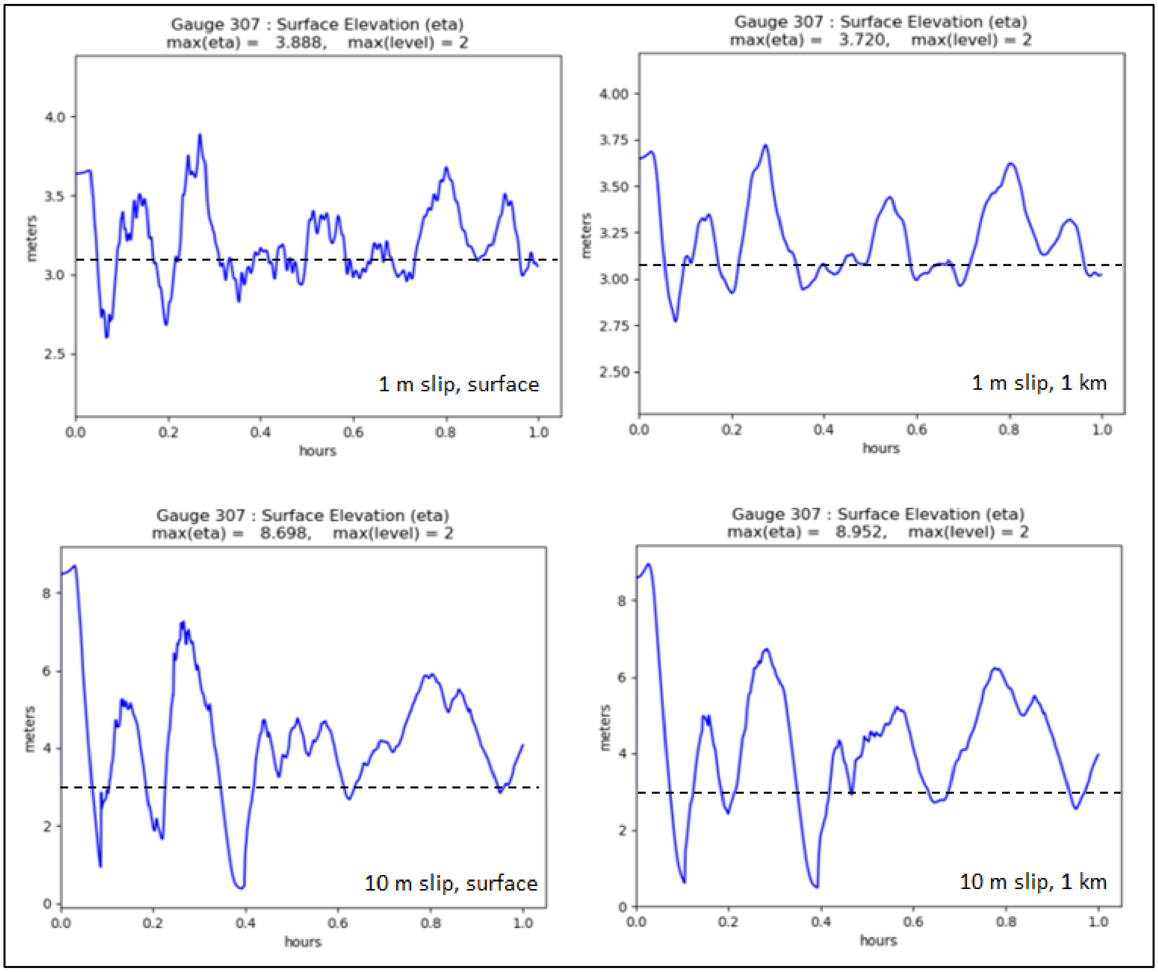

Figure 18. Gauge data taken from the maximum surface elevation time series for the four scenarios run with the modern-day lake level (black dotted line). Three of four runs recorded the highest surface elevation at gauge 307 (Andrews Bay). The 10-meter slip with a fault rupture at the surface is the only scenario with a maximum surface elevation greater by 0.1 meters at gauge 311 (Renton). Note change in vertical scale for bottom row vs. top row.

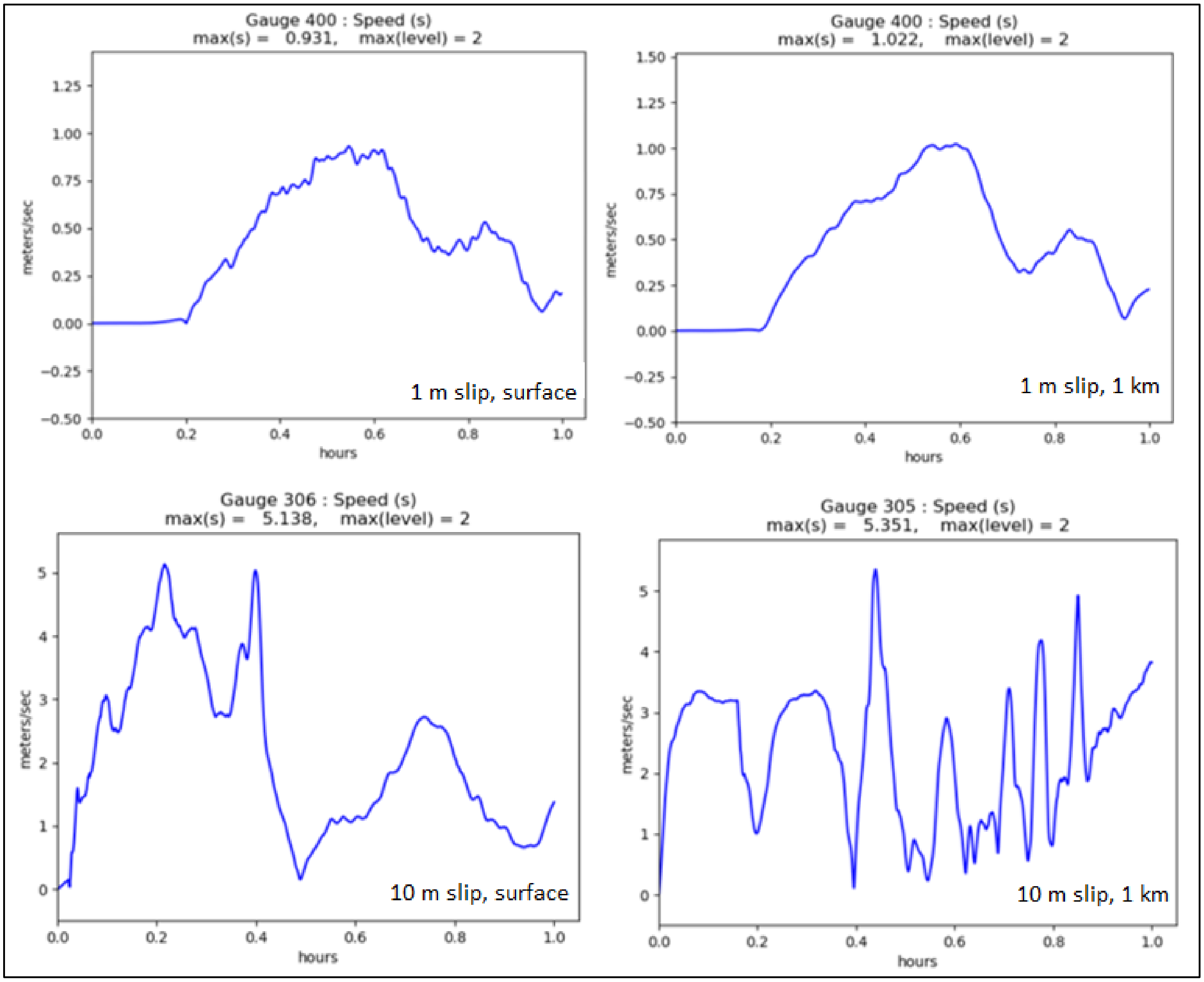

Figure 19. Gauge data taken from the maximum wave speed time series for the four scenarios run with the modern-day lake level. The 1-meter slip scenarios recorded their max wave speed at gauge 400, located at the entrance of the Montlake Cut to Portage Bay at t=0.6 hours. The 10-meter slip scenarios recorded their max wave speed at t=0.4 hours at gauge 306 (West of Mercer Island) for the fault rupture at the surface and gauge 307 (Andrews Bay) for the fault rupture at a depth of 1 km.

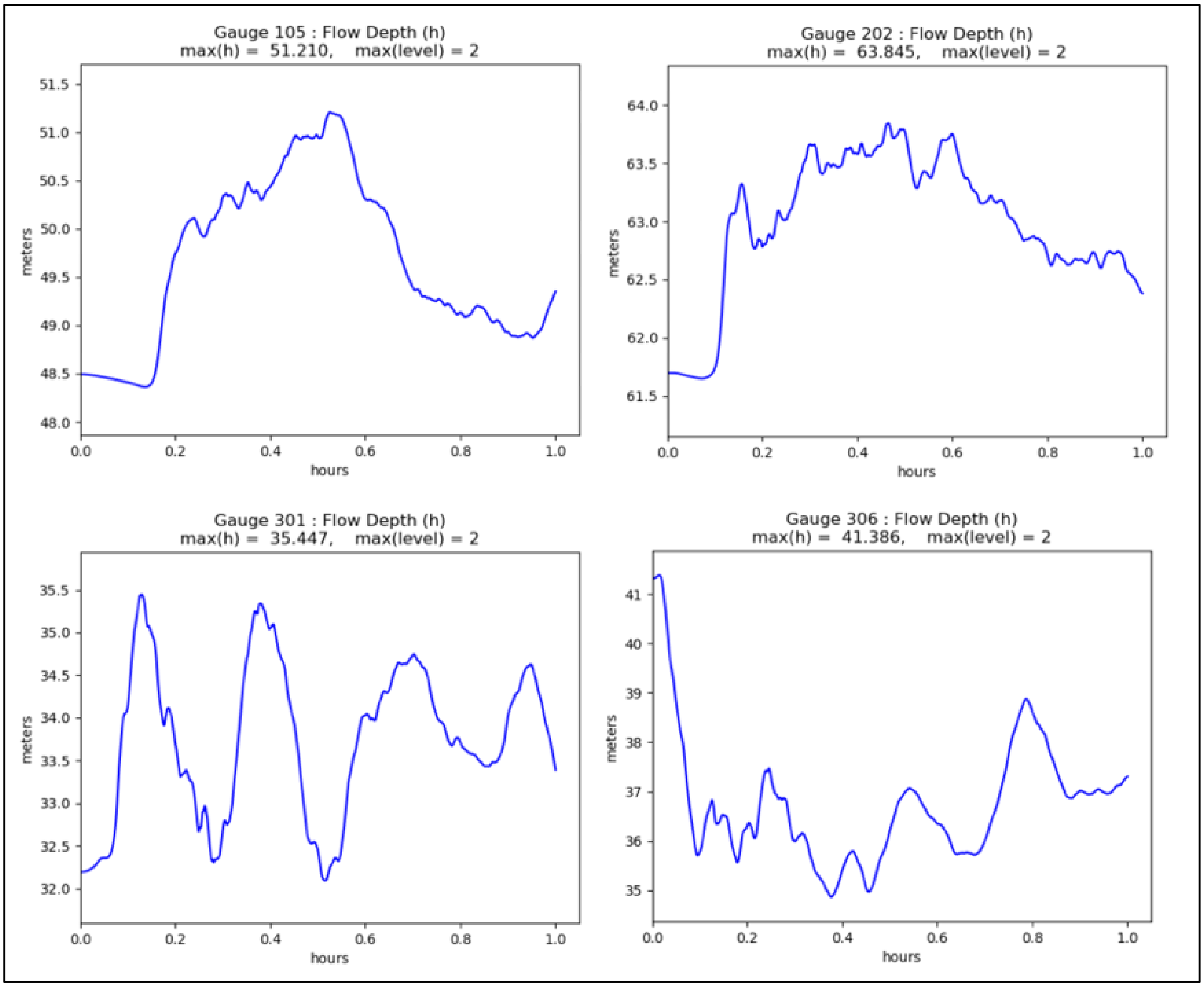

Figure 20. The gauges with the four highest flow depth values for the 10-meter slip with a fault rupture at 1 km depth is shown above. These values are representative for all four scenarios run.

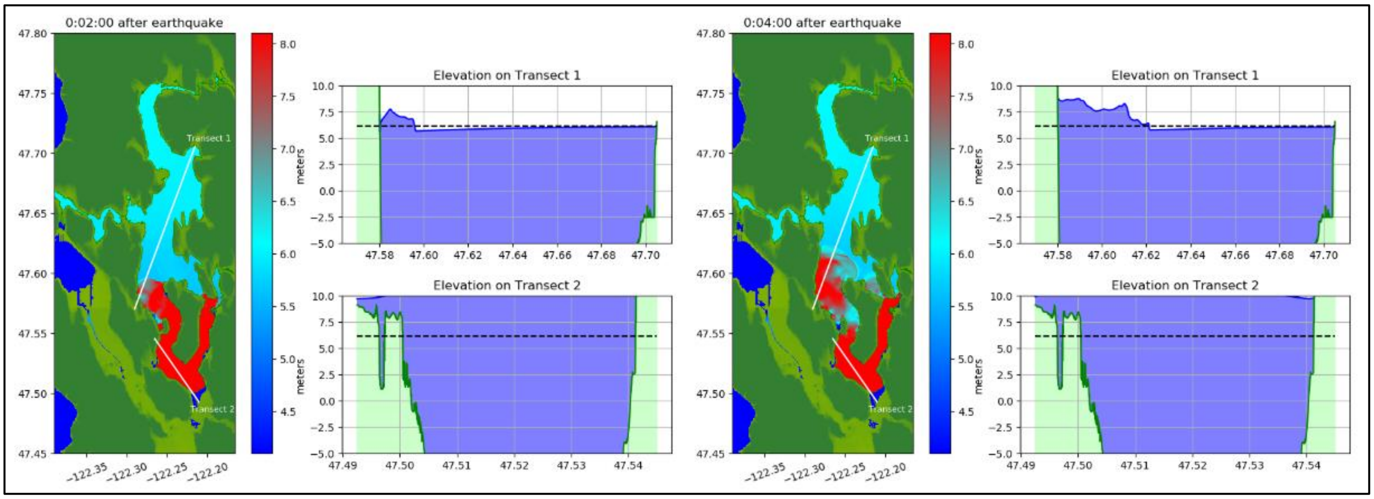

Figure 21. The 10-meter slip with a fault rupture at the surface scenario indicating surface wave elevation at t= 2 minutes on the left and t= 4 minutes on the right with an elevation of 2 meters north of the Seattle fault (Transect 1). Instantaneous uplift is seen south of the Seattle fault (Transect 2). The black dotted line indicates the initial lake level, set to 6.1 meters above MHW for the pre-ship canal lake level.

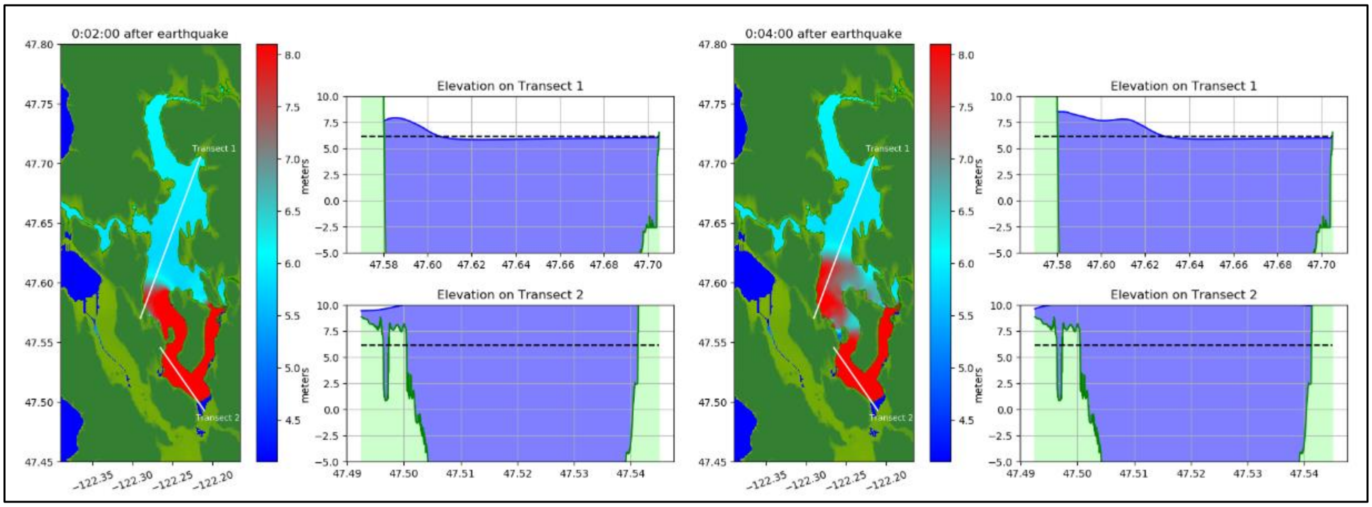

Figure 22. The 10-meter slip with a fault rupture at a depth of 1 km scenario indicating surface wave elevation at t= 2 minutes on the left and t= 4 minutes on the right with an elevation of 2 meters north of the Seattle fault (Transect 1). Instantaneous uplift is seen south of the Seattle fault (Transect 2). The black dotted line indicates the initial lake level, set to 6.1 meters above MHW for the pre-ship canal lake level.

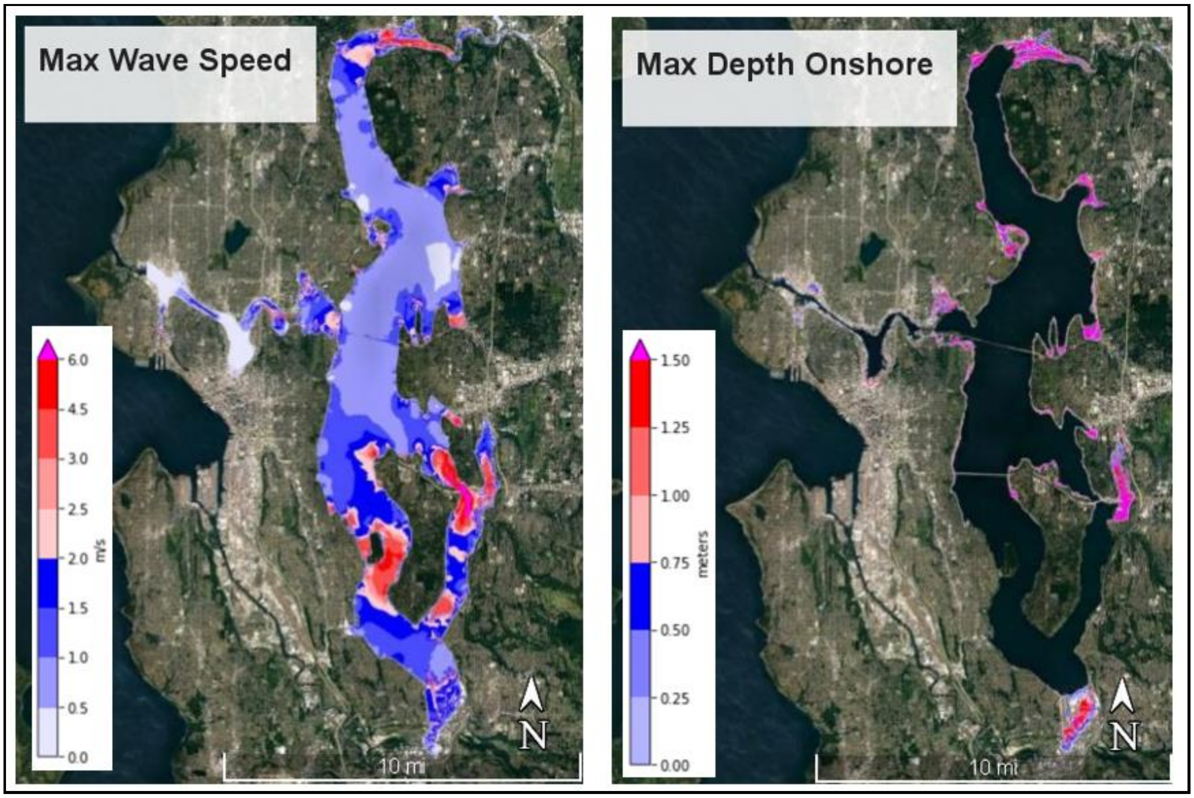

Figure 23. The Max Wave Speed plot (left) shows the maximum speed at each fgmax point. Regions colored blue or red are either offshore (initially wet) or onshore points that got wet, colored by the maximum water speed $s=\sqrt{(u^2+v^2)}$ over the simulation. The Max Depth Onshore plot (right) shows the maximum flow depth over the eight-hour simulation. Regions colored blue or red are initially dry fgmax points that did get wet during the tsunami, with color showing the maximum depth of water recorded.

Location	Gauge Number	Highest Surface Elevation from Lake Level (m)	Number of Inundations	Max Wave Speed (m/s)
Kenmore Waterfront	101	3.9	4	1.918
Juanita Beach Park	103	2.7	4	1.376
Matthews Beach Park	104	3.1	4	0.617
Magnason Park	200	2.2	4	2.045
Kirkland Waterfront	201	2.4	4	1.356
Yarrow Bay	203	3.1	4	1.383
Fairweather Bay	204	3.4	4	2.013
UW, low-lying	205	2.2	3	0.8

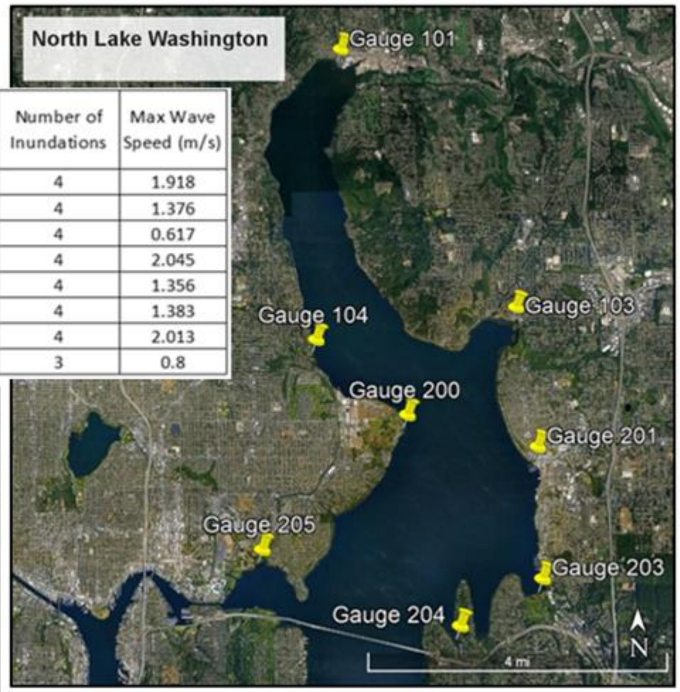

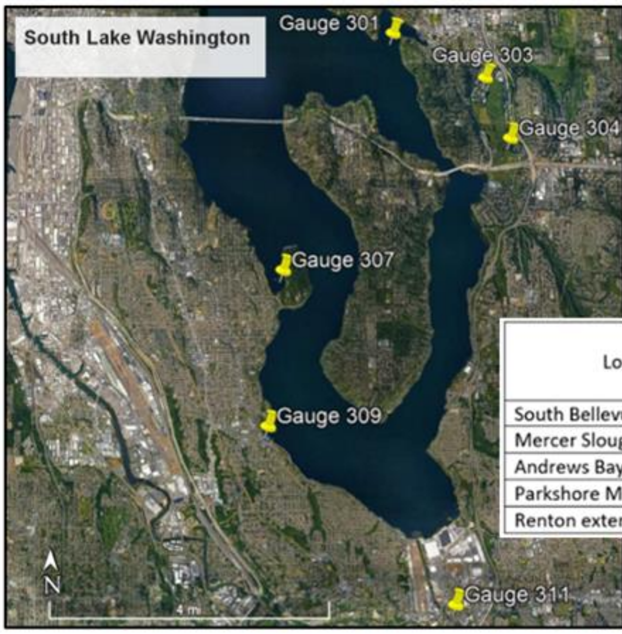

Location	Gauge Number	Highest Surface Elevation from Lake Level (m)	Number of Inundations	Max Wave Speed (m/s)
South Bellevue	303	1.8	4	1.477
Mercer Slough Nature Park	304	1.9	2	6.059
Andrews Bay	307	5.8	1	2.715
Parkshore Marina	309	4.7	4	2.505
Renton extent	311	5.6	4	2.115

Figure 24. Location map of the north and south regions of Lake Washington. Gauges shown here report data for areas of potential inundation. Surface elevation data and number of inundations are taken from the surface wave depth plots. The max wave speed data is taken from the max wave speed plots for each gauge location.

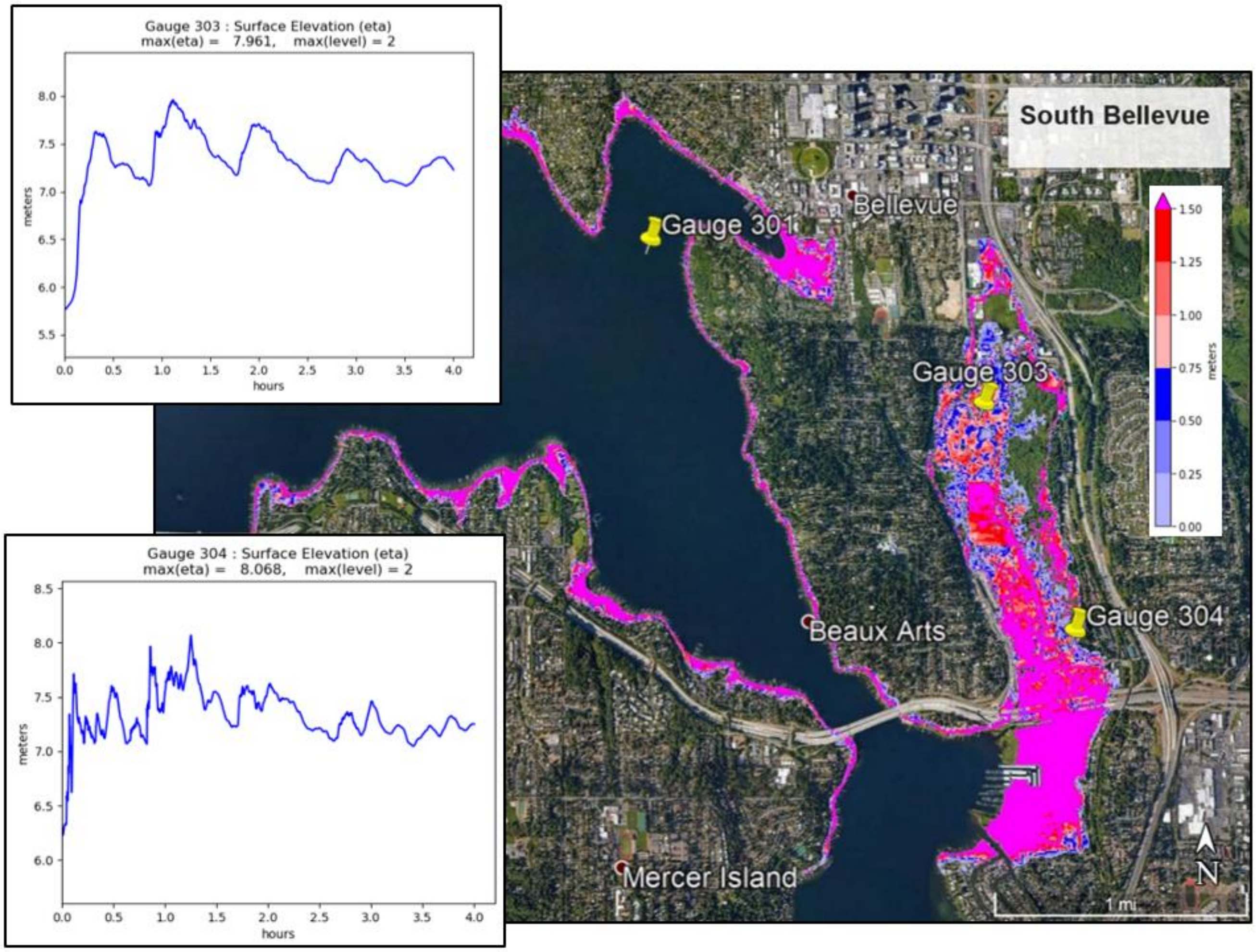

Figure 25. Gauges located in the South Bellevue area indicate potential areas of inundation. Surface elevation data from gauges 303 and 304 indicate inundation in the low-lying area of the Mercer Slough Nature Park.

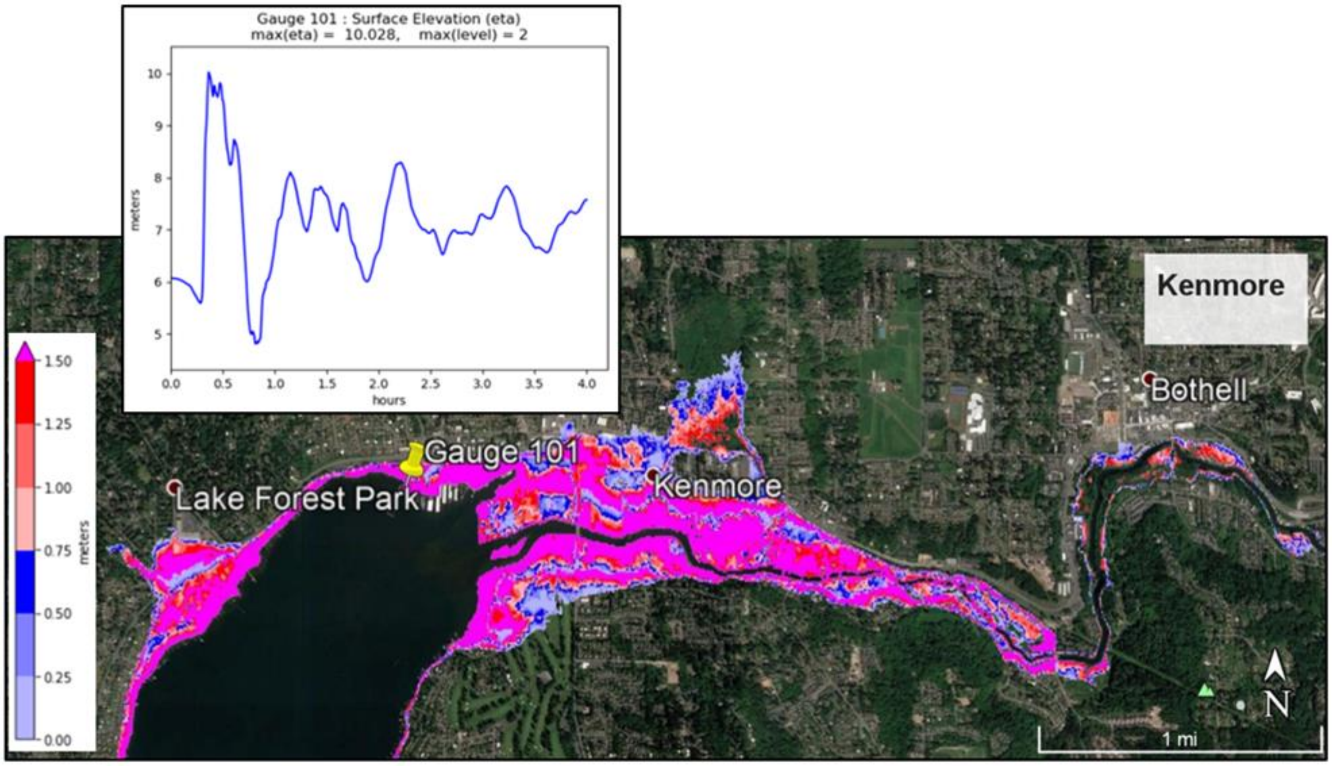

Figure 26. Gauges located in the Kenmore area indicate potential areas of inundation. Surface elevation data from gauge 101 display inundation in the low-lying areas of the Kenmore Waterfront and along the Sammamish River.

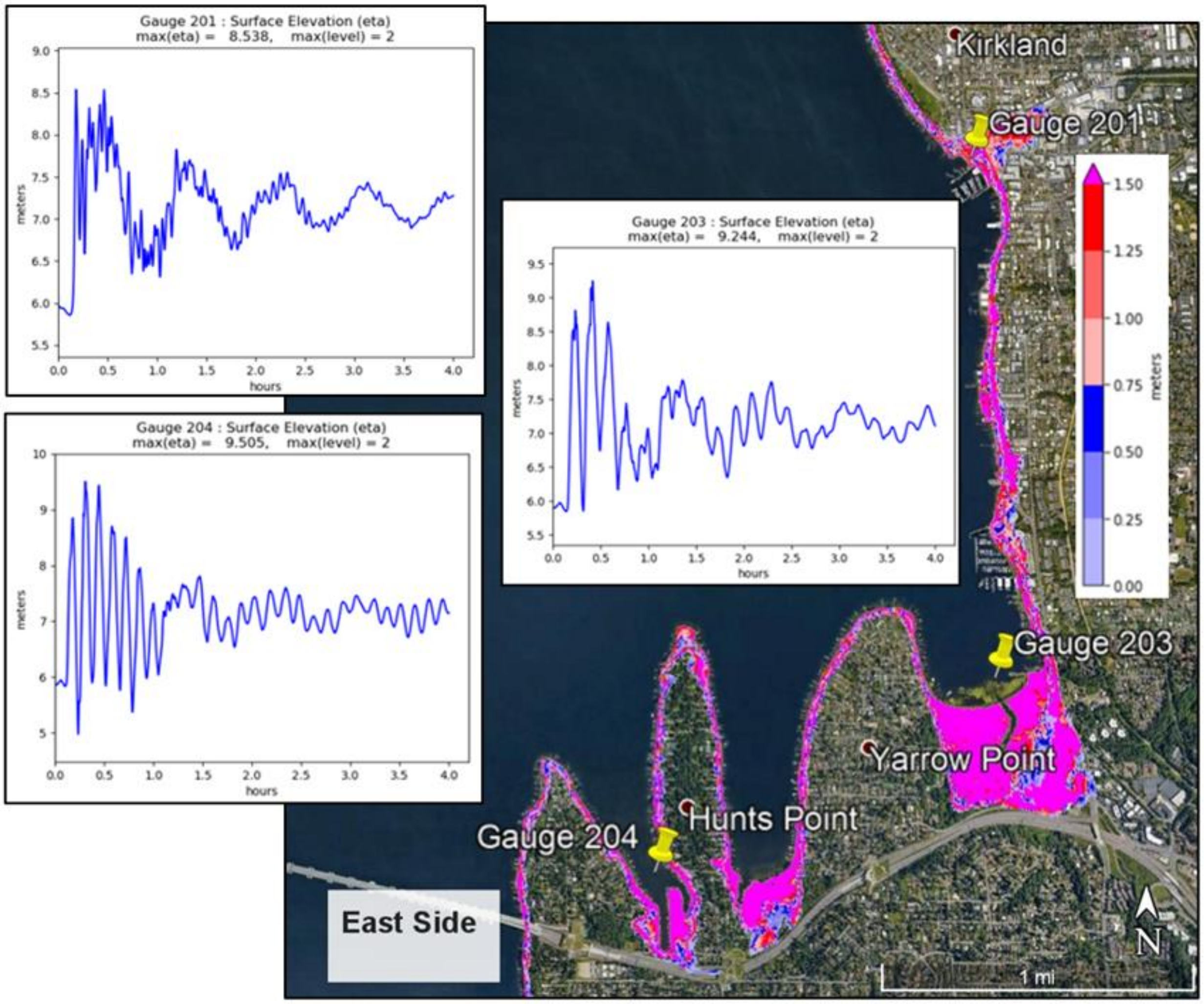

Figure 27. Gauges located on the east side of Lake Washington (in the vicinity of Kirkland) indicate potential areas of inundation. Surface elevation data from gauges 201, 203 and 204 display inundation around the low-lying areas of the Kirkland Waterfront (201), Yarrow Bay (203) and Fairweather Bay (204).

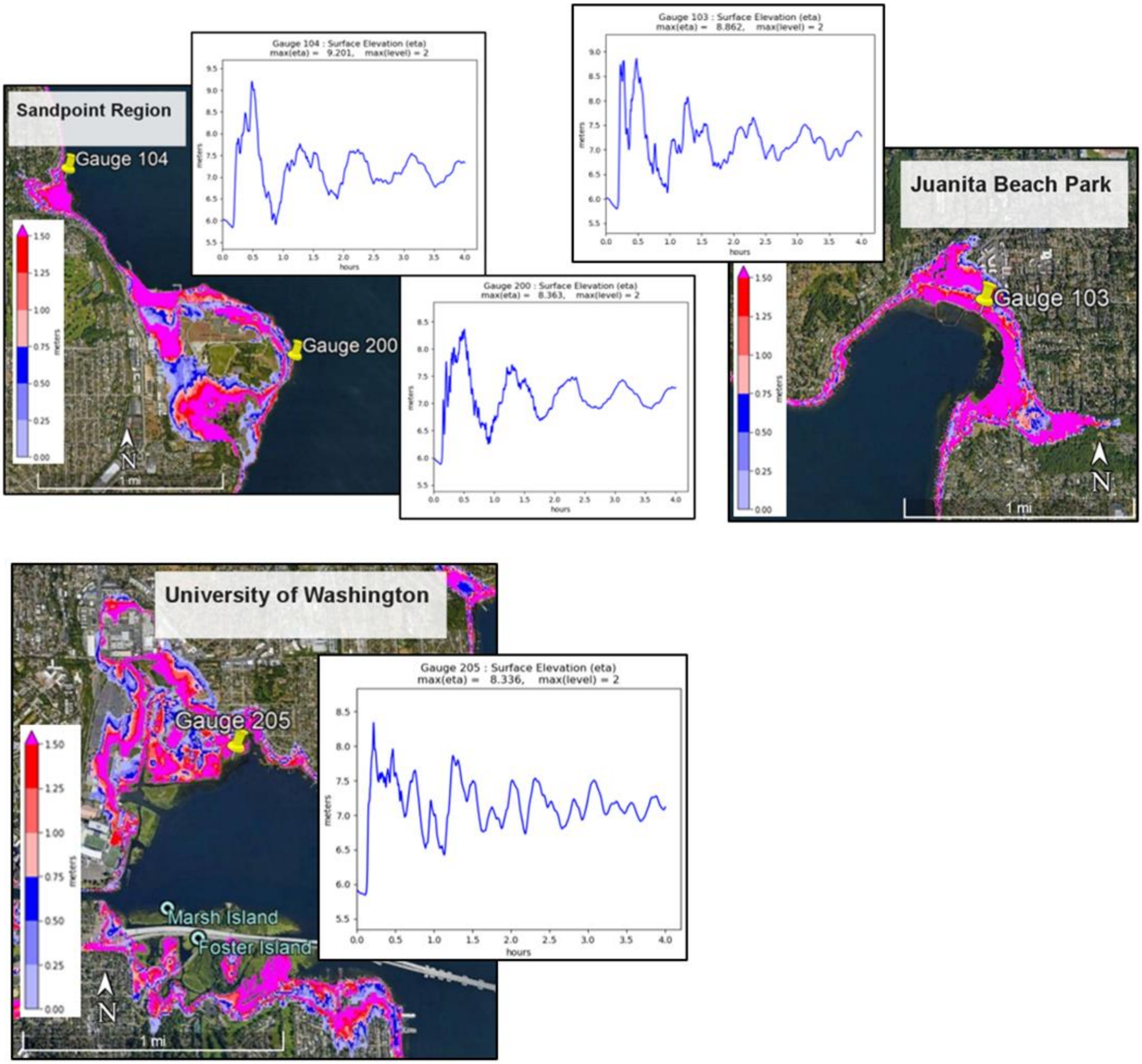

Figure 28. Gauges located in the Sandpoint Region, Juanita Beach Park and the University of Washington indicate potential areas of inundation. Surface wave elevation data from Matthews Beach Park (104) and Magnuson Park (200) display inundation around the Sandpoint Region with four inundation events. Gauge 103 located at Juanita Beach Park and gauge 205 located at the University of Washington displays surface wave elevation data indicative of inundation.

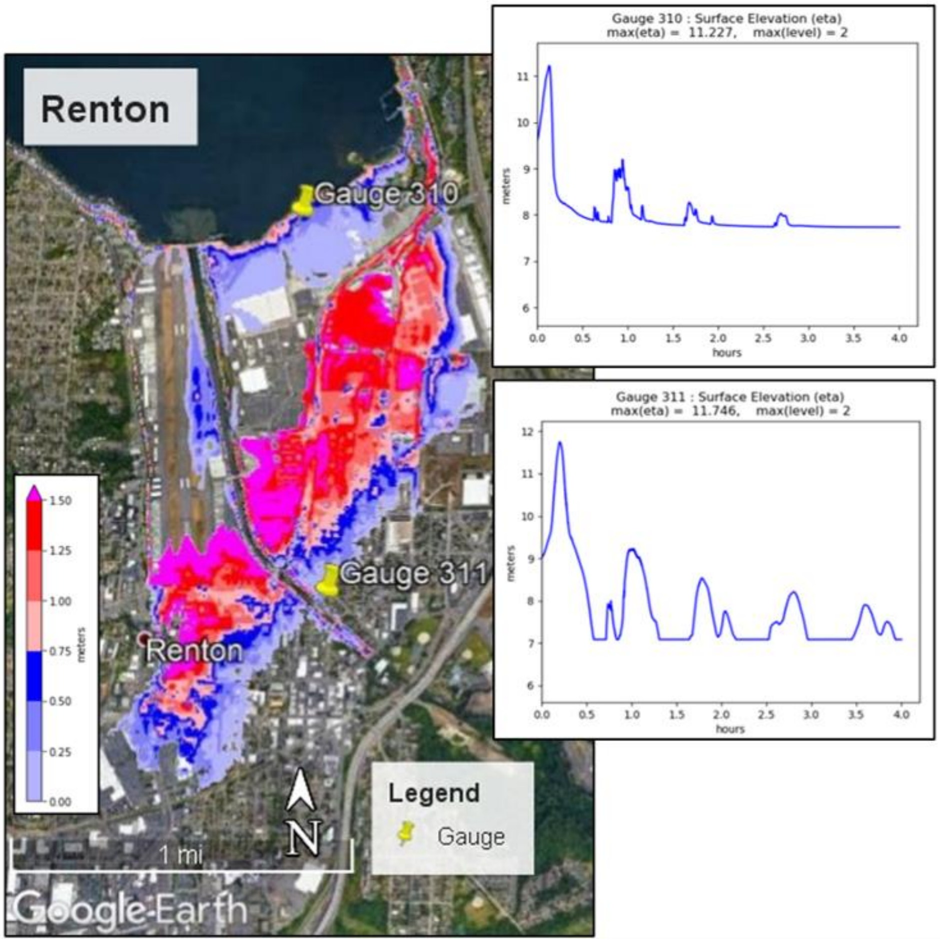

Figure 29. Gauges located in Renton indicate potential areas of inundation. Surface wave elevation data from Renton (310) and Renton extent (311) display inundation around the waterfront area with four inundation events. Gauge 310 located on the shoreline and gauge 311 located inland 1.9 km displays surface wave elevation data indicative of inundation.

Table 1. Seattle fault extent taken from Johnson et al. (1999).

Extent	Latitude	Longitude
West end	47.571274°	-122.342014°
East end	47.589295°	-122.078763°

Table 2. Deformation files created with Jupyter Notebooks. All files were used in the scenario testing to determine which scenario will be run for the full modelling length.

Deformation File Name	Slip	Depth	Lake Level
SFfaultLakeWA_1m_slip_1km.tt3	1 m	1 km	3.1 m above MHW
SFfaultLakeWA_1m_slip_surface.tt3	1 m	1 m	3.1 m above MHW
SFfaultLakeWA_10m_slip_1km.tt3	10 m	1 km	3.1 m above MHW
SFfaultLakeWA_10m_slip_surface.tt3	10 m	1 m	3.1 m above MHW
SFfaultLakeWA_1m_slip_1km_precanal.tt3	1 m	1 km	6.1 m above MHW
SFfaultLakeWA_1m_slip_surface_precanal.tt3	1 m	1 m	6.1 m above MHW
SFfaultLakeWA_10m_slip_1km_precanal.tt3	10 m	1 km	6.1 m above MHW
SFfaultLakeWA_10m_slip_surface_precanal.tt3	10 m	1 m	6.1 m above MHW

Table 3. The four scenarios run with the modern-day lake level results summary are shown below. The maximum surface displacement of the lake bottom due to the fault slip, maximum and minimum wave speeds, surface wave elevation above the normal lake level (depth), and flow depth values (including the initial water depth) taken from gauges located within the Lake Washington study area.

Scenario	Mw	Max Surface Displacement (m)	Max Speed (m/s)	Min Speed (m/s)	Max Depth (m)	Min Depth (m)	Max Flow Depth (m)	Min Flow Depth (m)
1m_slip_surface	6.78	0.57	0.93	0.014	3.8	3.2	61.9	0.58
1m_slip_1km	6.78	0.59	1.02	0.012	3.7	3.3	61.9	0.54
10m_slip_surface	7.45	5.65	5.13	0.087	8.7	3.9	63.7	0.32
10m_slip_1km	7.45	5.92	5.30	0.085	8.9	3.7	63.8	0.25

Table 4. The four scenarios run with the pre-ship-canal lake level results summary are shown below. The maximum surface displacement of the lake bottom due to the fault slip, maximum and minimum wave speeds, surface wave elevation above the normal lake level (depth), and flow depth values (including the initial water depth) taken from gauges located within the Lake Washington study area.

Scenario	Mw	Max Surface Displacement (m)	Max Speed (m/s)	Min Speed (m/s)	Max Depth (m)	Min Depth (m)	Max Flow Depth (m)	Min Flow Depth (m)
1m_slip_surface	6.78	0.57	0.91	0.080	6.8	6.2	64.9	1.3
1m_slip_1km	6.78	0.59	1.00	0.031	6.6	6.2	64.9	1.2
10m_slip_surface	7.45	5.65	6.24	0.620	11.7	7.9	66.6	3.1
10m_slip_1km	7.45	5.92	5.77	0.061	11.9	7.6	66.7	3.4

Table 5. The extended scenario run results summary is shown below (10 m of slip on a fault 1 km below the surface, with pre-ship-canal lake levels). The maximum surface displacement of the lake bottom due to the fault slip, maximum and minimum wave speeds, surface wave elevation above the normal lake level (depth), and flow depth values (including the initial water depth) taken from gauges located within the Lake Washington study area.

Scenario	Mw	Max Surface Displacement (m)	Max Speed (m/s)	Min Speed (m/s)	Max Depth (m)	Min Depth (m)	Max Flow Depth (m)	Min Flow Depth (m)
10m_slip_1km	7.45	5.92	6.05	0.61	11.9	7.7	66.7	2.8